

1 **The Transient Variation of the Complexes of the Low Latitude Ionosphere within the**  
2 **Equatorial Ionization Anomaly Region of Nigeria.**

3 **A. B. Rabi<sup>1,2</sup>, B. O. Ogunsua<sup>1</sup>, I. A. Fuwape<sup>1</sup> and J. A. Laoye<sup>3</sup>**

4 [1] {Space Physics Laboratory, Department of Physics, Federal University of Technology,  
5 Akure, Ondo State, Nigeria}

6 [2]{Centre for Atmospheric Research, National Space Research and Development Agency,  
7 Anyigba, Kogi State Nigeria}

8 [3] {Department of Physics, Olabisi Onabanjo University, Ago-Iwoye, Ogun State, Nigeria}

9

10 Correspondence to: B. O. Ogunsua (iobogunsua@futa.edu.ng)

11

12 **Abstract**

13 The quest to find an index for proper characterization and description of the dynamical response  
14 of the ionosphere to external influences and its various internal irregularities has led to the study  
15 of the day to day variations of the chaoticity and dynamical complexity of the ionosphere. This  
16 study was conducted using Global Positioning System (GPS) Total Electron Content (TEC) time  
17 series, measured in the year 2011, from 5 GPS receiver stations in Nigeria which lies within the  
18 Equatorial Ionization Anomaly region. The nonlinear aspect of the TEC time series were  
19 obtained by detrending the data. The detrended TEC time series were subjected to various  
20 analyses to obtain the phase space reconstruction and to compute the chaotic quantifiers which  
21 are Lyapunov exponents LE, correlation dimension, and Tsallis entropy for the study of  
22 dynamical complexity. Considering all the days of the year the daily/transient variations show no  
23 definite pattern for each month but day to day values of Lyapunov exponent for the entire year  
24 show a wavelike semiannual variation pattern with lower values around March, April, September  
25 and October, a change in pattern which demonstrates the self-organized critical phenomenon of  
26 the system. This can be seen from the correlation dimension with values between 2.7 and 3.2  
27 with lower values occurring mostly during storm periods demonstrating a phase transition from  
28 higher dimension during the quiet periods to lower dimension during storms for most of the  
29 stations. The values of Tsallis entropy show similar variation pattern with that of Lyapunov  
30 Exponent, with both quantifiers correlating within the range of 0.79 to 0.82. These results show



31 that both quantifiers can be further used together as indices in the study of the variations of the  
32 dynamical complexity of the ionosphere. The presence of chaos and high variations in the  
33 dynamical complexity, even at quiet periods in the ionosphere may be due to the internal  
34 dynamics and inherent irregularities of the ionosphere which exhibit non-linear properties.  
35 However, this inherent dynamics may be complicated by external factors like Geomagnetic  
36 storms. This may be the main reason for the drop in the values of Lyapunov exponent and Tsallis  
37 entropy during storms. The dynamical behavior of the ionosphere throughout the year as  
38 described by these quantifiers, were discussed in this work.

39

## 40 **1.0 Introduction**

41 The behavior of natural systems like the ionosphere is a function of changes that occur in the  
42 underlying dynamics that exists in such system. These underlying dynamics however can be  
43 sometimes complex and nonlinear due to superposition of different changes in dynamical  
44 variables that constitute it. When the dynamical states of a system changes suddenly due to  
45 sudden changes in the external factor affecting the system, then such a system is said to be  
46 deterministic.

47 However, there is no totally deterministic system in nature, because all natural systems exhibit a  
48 mixture of both deterministic properties. Although few natural systems have been found to be  
49 low dimensional deterministic in the sense of the theory, the concept of low-dimensional chaos  
50 has been proven to be fruitful in the understanding of many complex phenomena (Hegger et al.,  
51 1999) The degree of determinism or stochasticity in most natural systems is dependent on how  
52 much the system can be influenced by external factors, the nature of these external factors among  
53 others .The ionosphere like every other natural system possess its intrinsic dynamics and it can  
54 also be influenced by other external factors. The typical characteristics of a dynamical system  
55 like the ionosphere is expected to naturally show the interplay between determinism and  
56 stochasticity simply because of the fact that the ionosphere which has an inherent internal  
57 dynamics is also influenced by the influx of stochastic drivers like the solar wind, since it is  
58 influenced by external dynamics like every other natural system. This has made pure  
59 determinism impossible in the ionosphere, a situation that is common to all natural system and its  
60 surrounding.



61 The intensity of the solar wind coming into the ionosphere varies with the solar activity and an  
62 **extreme** solar activity can lead to geomagnetic storms and substorms drive in high intensity  
63 plasma wind at enormous speed and it serves as major stochastic driver leading to storm. The  
64 solar wind is driven from the sun into the ionospheric system during the quiet and storm and  
65 during relatively quiet periods of each month of the year. However other processes which  
66 include various factors like local time variations of the neutral winds, ionization processes,  
67 production-recombination rates, photoionization processes, plasma diffusion and various  
68 electrodynamics processes. (Unnikrishnan, 2010). The mesosphere and the lower thermospheric  
69 dynamics as reported by Kazimirovsky and Vergasova (2009) and also the influence of gravity  
70 waves as reported by Sindelarova (2009) can also be of great influence on the internal dynamics  
71 of the ionosphere.

72 Therefore, it is of great importance to study the chaoticity and dynamical complexity of the  
73 ionosphere and its variations in all geophysical conditions. However a good number of  
74 investigations have been carried out on concept of chaos in the upper atmosphere before now  
75 which includes the study on magnetospheric dynamics and the ionosphere. The study of chaos in  
76 magnetospheric index time series such as AE and AL were initially carried out by (Vasiliadis et  
77 al., 1990, Shan et al, 1999; Pavlos et al, 1992). These previous efforts made by the  
78 aforementioned researchers has led to the development of the concept of investigating and  
79 revealing the chaoticity and the complex dynamics of the ionosphere, and as a result, studies on  
80 the chaoticity of the ionosphere have been conducted, by some investigators like Bhattacharyya  
81 (1990) who studied chaotic behavior of ionospheric diversity fluctuation using amplitude and  
82 phase scintillation data, and found the existence of low dimension chaos. Also, Wernik and Yeh  
83 (1994) further revealed the chaotic behavior of the ionospheric turbulence using scintillation data  
84 and numerical modeling of scintillation at high latitude. They showed that the ionospheric  
85 turbulence attractor (if it exists) cannot be reconstructed from amplitude scintillation data and  
86 their measured phase scintillation data adequately reproduce the assumed chaotic structure in the  
87 ionosphere. Also Kumar et al., (2004) reported the evidence of chaos in the ionosphere by  
88 showing the chaotic nature of the underlying dynamics of the fluctuations of TEC power  
89 spectrum indicating exponential decay and the calculated positive value of Lyapunov exponent.  
90 This is also supported by the results of the comparison of the chaotic characteristics of the time  
91 series of variations of TEC with the pseudochaotic characteristic of the colored noise time series.

92 Xuann et al., (2006) studied chaos properties of ionospheric total electron content (TEC) using  
93 TEC data from 1996 to 2004, and analyze possibility to predict it by using chaos. They found  
94 the presence of chaos in the TEC measured in the study area, as indicated by the positive  
95 Lyapunov exponent computed from their data. The correlation dimension was 3.6092 from their  
96 estimation. They were also able to show that the TEC time series can be predicted using chaos.

97

98 Also, Unnikrishnan et al (2006a,b) have analyzed the deterministic chaos in mid latitude and  
99 Unnikrishnan (2010), Unnikrishnan and Ravindran (2010), analyzed some TEC data from some  
100 Indian low latitude stations for quiet period and major storm period and found in Their results the  
101 presence of chaos which was indicated by a positive Lyapunov exponent, and they also inferred  
102 that storm periods exhibits lower values compared to quiet periods. The dynamical complexity  
103 of magnetospheric processes and the ionosphere have been studied by a number of researchers.  
104 Balasis et al., (2008) investigated the dynamical complexity of the magnetosphere by using  
105 Tsallis entropy as a dynamical complexity measure in  $D_{st}$  time series also Balasis et al., (2009)  
106 investigated the dynamical complexity in  $D_{st}$  further by considering different entropy measures.  
107 Coco et al (2011) using the information theory approach studied the dynamical changes of the  
108 polar cap potential which is characteristic of the polar region ionosphere by considering three  
109 cases (i) steady IMF  $B_z > 0$ , (ii) steady IMF  $B_z < 0$  and (iii) a double rotation from negative to  
110 positive and then positive to negative  $B_z$ . They observed a neat dynamical topological transition  
111 when the IMF  $B_z$  turns from negative to positive and vice versa, pointing toward the possible  
112 occurrence of an order/disorder phase transition, which is the counterpart of the large scale  
113 convection rearrangement and of the increase of the global coherence. Further studies in chaotic  
114 behavior and nonlinear dynamics is however needed to improve our understanding of the  
115 dynamical behavior of the ionosphere of low latitude ionosphere especially over Africa during  
116 quiet and storm for different season of the year some as to be able to characterize chaoticity for  
117 different season of the year for quiet and storm periods. Recently Ogunsua et al (2014) studied  
118 comparatively the chaoticity of the equatorial ionosphere over Nigeria using TEC data,  
119 considering five quietest day classification and five most disturbed day classification. They were  
120 able to show the presence of chaos as indicated the positive Lyapunov exponents and also were  
121 able to show that Tsallis entropy can be used as a viable measure of dynamical complexity in the



122 ionosphere with portions showing lower values of Tsallis entropy indicating lower dynamical  
123 complexity, with a good relationship with Lyapunov exponents. They found a phase transition  
124 from higher dimension during quiet days to Lower dimension during storm.

125

126 The low latitude region where Nigeria is situated is known as the equatorial anomaly region,  
127 where **the magnetic field B is almost totally parallel to the equator**. Off the equator the E region  
128 electric field **maps map** along the magnetic field up to the F-region altitude in the low latitude,  
129 this eastward electric field (E) interacts with the magnetic field B at the F region during the day.  
130 This results in the electrodynamic lifting of the F-region plasma over the equator, known as  
131 EXB drift. The uplifted plasma over the equator moves along the magnetic line in response to  
132 gravity, diffusion and pressure gradients and hence, the fountain effect. The fountain effect being  
133 controlled by the EXB drift shows the dynamics of the diurnal variation equatorial anomaly  
134 (Abdu, 1997; Unnikrishnan 2010). There is a reduction in the F region ionization density at the  
135 magnetic equator and also much enhanced ionization density at the two anomaly crests within  
136  $\pm 15^\circ$  of the magnetic latitude north and south of the equator (Rama Rao et al., 2006). The  
137 equatorial ionization anomaly and other natural processes which includes various ionization  
138 processes and recombination; influx of solar wind, photoionization processes and so many other  
139 factors that occur due to variations in solar activities, have a great influence on the systems of  
140 the ionosphere, due to their effects on internal dynamics of the ionosphere. This portrays the  
141 ionosphere as a typical natural system with continuous interaction with its external environment  
142 which led to the study of the influence of the sun on the ionosphere (Ogunsua et al., 2014).

143 The ionosphere possesses a significant level of nonlinear variations that requires more  
144 investigation which can be studied and characterized using nonlinear approach like the chaoticity  
145 and dynamical complexity for the study of its dynamics. The need to study the daily variation in  
146 the dynamical complexity of the ionosphere arises from the established knowledge and  
147 understanding which shows that the ionosphere is a complex system with so many variations that  
148 can arise from various dynamical changes that can be due to various changes in different  
149 processes that contribute to the behavior and nature of the ionosphere. Rabiou et al., (2007)  
150 affirmed that characterizing the ionosphere is of utmost importance due to the numerous  
151 complexities associated with the region. The scale of these numerous complexities interestingly

152 changes at times from one day to another. The concept of chaos as applied to ionospheric and  
153 magnetospheric studies on quiet and stormy conditions are limited.

154 Most investigations have been based on only quiet and storm conditions for all studies carried  
155 out, and none of the previous works involved the quiet and disturbed day classification of  
156 geophysical conditions until recently by Ogunsua et al.,(2014), where we considered the  
157 comparative use of Lyapunov exponent and Tsallis entropy as proxies for the internal dynamics  
158 of the ionosphere. This is the main reason for the consideration of day to day variation of these  
159 parameters in this work.

## 160 **2.0 Data and Methodology**

161 The data used for this study is the global positioning system (GPS) total electron content (TEC)  
162 data obtained from 5 GPS satellite receiver stations. Table 1 shows the coordinates of the  
163 stations. These receivers take the measure of slant TEC within  $1m^2$  columnar unit of the cross  
164 section along the ray path of the satellite and the receiver which is given by

$$165 \quad STEC = \int_{receiver}^{Satellite} Ndl \quad (1)$$

166 The observation of the total number of free electron along the ray path are derived from the  
167 frequency  $L_1(1572.42 \text{ MHz})$  and  $L_2(1227.60 \text{ MHz})$  of Global Positioning System(GPS),that  
168 provide the relative ionosphere delay of electromagnetic waves travelling through the medium  
169 (Saito et al.,1998). The Slant TEC is projected to vertical TEC using the thin shell model  
170 assuming the height of 350m (Klobuchar,1986).

$$171 \quad VTEC = STEC \cdot \cos[\arcsin(R_e \cos \Theta / R_e + h_{max})] \quad (2)$$

172 Where  $R_e = 6378km$  (radius of the earth),  $h_{max} = 350km$  (the vertical height assumed from  
173 the satellite) and  $\Theta = \text{elevation angle at ground station}$

174

175 In this study, 5 GPS TEC measuring stations lying within the low latitude region were  
176 considered, as shown in table 1. The TEC data obtained for January to December 2011 were  
177 considered for this study and the data are given at 1min sampling time. The TEC data were

178 subjected to various analyses which will be discussed in the next section. The day to day  
179 variations of the chaotic behavior and dynamical complexity were studied for the entire year.  
180 The surrogate data tests for nonlinearity were also conducted for both the dynamical and  
181 geometrical aspects.

### 182 **3.0 Methods of Data Analysis and Results**

#### 183 **3.1 Time series analysis**

184 Time series can be seen as a numerical account that describes the state of a system, from which it  
185 was measured. A given time series,  $S_n$  can be defined as a sequence of scalar measurement of a  
186 particular quantity taken as series at different portion in time for a given time interval( $\Delta t$ ). The  
187 time series describe the physical appearance of an entire system, as seen in Fig 1. However it  
188 may not always describe the internal dynamics of that system. A system like the ionosphere  
189 possesses a dominant dynamics that can be seen as diurnal so the data should be treated so as to  
190 be able to see its internal dynamics. The measured TEC time series were plotted to see the  
191 dynamics of the system. A typical plot of TEC usually has a dominant dynamics (see fig 1)  
192 which may be seen as the diurnal behavior, however, it can also be seen that there is also a  
193 presence of fluctuations (which appear to be nonlinear) in the system as a result of the internal  
194 dynamics of the ionosphere and space plasma system, due to different activities in the  
195 ionosphere. Therefore there is need to minimize the influence of the diurnal variations since we  
196 are more interested in the nonlinear internal dynamics of the system in this study, to do so the  
197 TEC time series was detrended by carrying out the following analysis below:

198 Since for the given daily data of 1minute sampling time there are 1440 data points per day. Then  
199 there exists a time series  $t_i$ , where  $i = 1,2,3 \dots 1440$  represents the observed time series, and  
200 there also exists a set of  $u_i$  where  $i = 1,2,3 \dots 1440$ , such that the diurnal variation reduced time  
201 is given by

$$202 \quad T_i = t_i - u_j \quad (3)$$

203 Where  $i = 1,2,3, \dots, j = \text{mod}(i, 1440)$ , if  $\text{mod}(j, 1440) \neq 0$ , and  $j = 1440$  if  $d(j, 1440) = 0$ .  
204 This method will give the detrended time series represented by  $T_i$  obtained from the original

205 TEC data as shown in fig 2. This method is similar to that used by (Unnikrishnan et al., 2006,  
206 Unnikrishnan 2010), the further explanations on the dynamical results can be found in (Kumar et  
207 al., 2004). The detrended time series were subjected to further analyses for the Phase space  
208 reconstruction and also to obtain the values of Lyapunov exponents, correlation dimension,  
209 Tsallis entropy and the implementation of surrogate data test.

210

### 211 **3.1.1 Phase Space reconstruction and Non Linear Time Series Analysis**

212 The study of chaoticity and dynamical complexity in a dynamical system requires a nonlinear  
213 approach, due to the fact that systems described by these phenomena can be referred to as  
214 nonlinear complex systems. The magnetosphere and the ionosphere are good examples of such  
215 systems. To be able to study such phenomena some nonlinear time series analysis can be carried  
216 out on the time series data describing such a system. The detrended time series of TEC  
217 measurement is subjected to some nonlinear time series data analysis to obtain the mutual  
218 information and false nearest neighbours, embedding dimension and delay coordinates for the  
219 phase space reconstruction, and the evaluation of other chaotic quantifiers namely: Lyapunov  
220 Exponents, Correlation dimension, recurrence analysis and Entropy.

221 The phase space reconstruction helps to reveal the multidirectional aspect of the system. The  
222 phase space reconstruction is based on embedding theorem, such that the phase space is  
223 reconstructed to show the multidimensional nature as follows:

$$224 \quad Y_n = (s_{n-(m-1)\tau}, s_{n-(m-2)\tau}, \dots, s_{n-\tau}, s_n) \quad (4)$$

225 where  $Y_n$  are vector in phase space. The proper choice of embedding dimension ( $m$ ) and delay  
226 Time ( $\tau$ ) are essential for phase space reconstruction (Fraser and Swinney,1986; Kennel et  
227 al.,1992) .

228 If the plot showing the time delayed mutual information shows a marked minimum that value  
229 can be considered as a responsible time delay; Fig 3 shows the mutual information plotted  
230 against time delay. Likewise, the minimal embedding dimension, which correspond to the  
231 minimum number of the false nearest neighbours can be treated as the optimum value of



232 embedding dimension (Unnikrishnan et al.,2006, Unnikrishnan, 2010). A plot of fraction of false  
 233 nearest neighbours against embedding dimension can be seen in Fig 4. It was observed that for  
 234 all the daily detrended TEC time series the choice of  $\tau \geq 30$  and  $m \geq 4$  values of delay and  
 235 embedding dimension above these values are suitable for analysis of data for all stations. The  
 236 choice of  $\tau = 30$  and  $m = 5$  were mostly used to analyze the dynamical aspects for all the  
 237 stations. The reconstructed Phase space trajectory is shown in Fig 5

### 238 3.1.2 Lyapunov Exponents

239 The Lyapunov exponent has been a very important quantifier for the determination of chaos in a  
 240 dynamical system. This quantifier is also used for the determination of chaos in time series,  
 241 representing natural systems like the ionosphere and magnetosphere (Unnikrishnan 2008, 2010).  
 242 A positive Lyapunov exponent indicates divergence of trajectory in one dimension, or alternative  
 243 an expansion of volume, which can also be said to indicate repulsion, or attraction from a fixed  
 244 point. A positive Lyapunov exponent indicates that there is evidence of chaos in a dissipative  
 245 deterministic system, where the positive Lyapunov exponent indicates divergence of trajectory in  
 246 one direction or expansion of value and a negative value shows convergence at trajectory or  
 247 contraction of volume along another direction.

248 The largest Lyapunov exponent ( $\lambda_1$ ) can be used to determine the rate of divergence as indicated  
 249 by (Wolf et al.,1985)

250 Where

$$251 \lambda_1 = \lim_{r \rightarrow \infty} \frac{1}{t} \ln \frac{\Delta x(t)}{x(0)} = \lim_{r \rightarrow \infty} \frac{1}{t} \sum_{i=1}^t \ln \left( \frac{\Delta x(t_i)}{\Delta x(t_{i-1})} \right) \quad (5)$$

252 The Lyapunov exponent was computed for the TEC values measured from Different stations.  
 253 The evolution in state space was scanned with  $\tau = 30$ ,  $m = 5$ , is shown in fig 6. The day to day  
 254 variations of the Lyapunov exponent was computed for the entire year to so as to study the  
 255 annual trend of variation. This was implemented using the method introduced by Rosenstein  
 256 (1993), and Hegger et al., (1994), both algorithms use very similar methods. Lyapunov  
 257 exponents were also computed for varying time delay at constant embedding dimension and also  
 258 for varying embedding dimension, to check for the stability with changes in trajectory. These can

259 be seen in fig. 6b and 6c. The day to day values of Lyapunov exponent plotted for the Enugu  
 260 station and for Toro station are shown in fig 7a to 7b. The plots of the day to day values show the  
 261 transient variation of the ionosphere and a wavelike yearly pattern.

### 262 3.1.3 Correlation Dimension

263 Another relevant method to study the underlying dynamics or internal dynamics of a system is to  
 264 evaluate the dimension of the system. The correlation dimension gives a good approximation of  
 265 this as suggested by Grassberger and Procaccia (1983a; b). The correlation dimension is  
 266 preferred over the box counting dimension because it takes into account the density of points on  
 267 the attractor (Strogatz 1994). The correlation dimension  $D$  is defined as

$$268 \quad D = \lim_{r \rightarrow 0} \frac{\ln C(r)}{\ln r} \quad (6)$$

269 The term  $C(r)$  is the correlation sum for radius ( $r$ ) where for a small radius ( $r$ ) the correlation  
 270 sum can be seen as  $C(r) \sim r^d$  for  $r \rightarrow 0$ . The correlation sum is dependent of the embedding  
 271 dimension ( $m$ ) of the reconstructed phase space and it is also dependent of the length of the time  
 272 series  $N$  as follows

$$273 \quad C(r) = \frac{2}{N(N-1)} \sum_{i=1}^N \sum_{j=i+1}^N \Theta(r - \|y_i - y_j\|) \quad (7)$$

274 Where  $\Theta$  is the Heaviside step function, with  $\Theta(H) = 0$  if  $H \leq 0$  and  $\Theta(H) = 1$  for  $H > 0$ .

275 The correlation dimension was computed using the Theiler algorithm approach, with Theiler  
 276 window ( $w$ ) at 180. The Theiler window was chosen to be approximately equal to the product of  
 277  $m$  and  $\tau$ . A similar approach to the computation of correlation dimension was used by  
 278 Unnikrishnan and Ravindran (2010) to determine the correlation dimension of detrended TEC  
 279 data for some stations in India which lies within the equatorial region, like Nigeria. Ogunsua et  
 280 al., (2014) also used similar methods for some detrended TEC from Nigerian stations.

281 The correlation dimension for data taken for the quietest day of October 2011 and the most  
 282 disturbed day of October 2011 from Birnin Kebbi GPS TEC measuring station were represented  
 283 by Fig 8a and Fig 8b respectively. The correlation dimension saturates at  $m \geq 4$  for the quietest  
 284 day of the month and at  $m \geq 5$  for the most disturbed day. In this illustration the most disturbed

285 day of this month fall within the storm period of October 2011. The classification of days into  
286 quiet and disturbed days in the month of October 2011 enables us to compare the quiet and storm  
287 periods together while comparing the quiet days with some relatively disturbed days.

### 288 **3.1.4 Computation of Tsallis Entropy and Principles of Nonextensive Tsallis Entropy**

289 Entropy measures are very important statistical techniques that can be used to describe the  
290 dynamical nature of a system. The Tsallis entropy can be used to describe the dynamical  
291 complexity of a system and to also understand the nonlinear dynamics like chaos which may  
292 exist in a natural system. The use of entropy measure as a method to describe the state of a  
293 physical system has been employed into information theory for decades. The computation of  
294 entropy allows us to describe the state of disorderliness in a system, one can generalize this same  
295 concept to characterize the amount of information stored in more general probability  
296 distributions (Kantz & Shrieber 2003, Balasis et al.,2009). The concept of information theory is  
297 basically concerned with these principles. The information theory gives us an important  
298 approach to time series analysis. If our time series which is a stream of numbers, is given as a  
299 source of information such that this numbers are distributed according to some probability  
300 distribution, and transitions between numbers occur with well-defined probabilities. One can  
301 deduce same average behaviour of the system at a different point and for the future. The term  
302 entropy is used in both physics and information theory to describe the amount of uncertainty or  
303 information inherent in an object or system (Kantz and schrieber 2003). The state of an open  
304 system is usually associated with a degree of uncertainty that can be quantified by the  
305 Boltzmann-Gibbs entropy, a very useful uncertainty measure in statistical mechanics. However  
306 Boltzmann-Gibbs entropy cannot, describe non-equilibrium physical systems with large  
307 variability and multifractal structure such as the solar wind (Burgala et al., 2007, Balasis et al.,  
308 2008). One of the crucial properties of the Boltzmann-Gibbs entropy in the context of classical  
309 thermodynamics is extensivity, namely proportionality with the number of elements of the  
310 system. The Boltzmann-Gibbs entropy satisfies this prescription if the subsystems are  
311 statistically (quasi-) independent, or typically if the correlations within the system are essentially  
312 local. In such cases the system is called extensive. In general however, the situation is not of this  
313 type and correlations may be far from negligible at all scales. In such cases, the Boltzmann-  
314 Gibbs entropy is nonextensive (Balasis et. al., 2008, 2009). These generalizations above were

315 proposed by Tsallis (1988), who was inspired by the probabilistic description of multifractal  
 316 geometries. Tsallis (1988, 1998) introduced an entropy measure by presenting an entropic  
 317 expression characterized by an index  $q$  which leads to a nonextensive statistics,

$$318 \quad S_q = k \frac{1}{q-1} \left( 1 - \sum_{i=1}^W p_i^q \right) \quad (8)$$

319 Where  $p_i$  are the probabilities associated with the microscopic configurations,  $W$  is their total  
 320 number,  $q$  is a real number, and  $k$  is Boltzmann's constant. The value  $q$  is a measure of the  
 321 nonextensivity of the system:  $q \rightarrow 1$  corresponds to the standard extensive Boltzmann-Gibbs  
 322 statistics. This is the basis of the so called nonextensive statistical mechanics, which generalizes  
 323 the Boltzmann-Gibbs theory. The entropic index  $q$  characterizes the degree of nonadditivity  
 324 reflected in the following pseudoadditivity rule:

$$325 \quad \frac{S_q(A+B)}{k} = \left[ \frac{S_q(A)}{k} \right] + \left[ \frac{S_q(B)}{k} \right] + (1 - q) \left[ \frac{S_q(A)}{k} \right] \left[ \frac{S_q(B)}{k} \right]. \quad (9)$$

326 The cases  $q > 1$  and  $q < 1$ , correspond to subadditivity (or subextensivity) and superadditivity  
 327 (or superextensivity), respectively and  $q = 1$  represents additivity (or extensivity). For  
 328 subsystems that have special theory probability correlations, extensivity is not a valid for  
 329 Boltzmann-Gibbs entropy in such cases, but may occur for  $S_q$  with a particular value of the index  
 330  $q$ . Such systems are sometimes referred to as nonextensive (Boon and Tsallis, 2005, Balasis et al  
 331 2008, 2009). The parameter  $q$  itself is not a measure of the complexity of the system, but  
 332 measures the degree of nonextensivity of the system. It is the time variations of the Tsallis  
 333 entropy for a given  $q(S_q)$  that quantify the dynamic changes of the complexity of the system.  
 334 Lower  $S_q$  values characterize the portions of the signal with lower complexity. In this  
 335 presentation we estimate  $S_q$  on the basis of the concept of symbolic dynamics and by using the  
 336 technique of lumping (Balasis et al. 2008, 2009).

337 A comparison of Tsallis entropy with Lyapunov exponents computed for the same set of data has  
 338 been carried out in this work, to see the efficacy of the combined usage of both parameters. This  
 339 is based on the established facts that variations in the values of Tsallis entropy can be linked with  
 340 that of Lyapunov exponents chaotic behavior in systems as seen in (Baranger et al., 2012;  
 341 Anastasiadis et al., 2005; Kalogeropoulos et al., 2012;2013). Coraddu et al., (2005) showed the

342 Tsallis entropy generalization for Lyapunov exponents. Further details can be found in Ogunsua  
343 et al., (2014),

344 they were able to investigate the similarities in their response to the complex dynamics of the  
345 ionosphere, and this informs the further use of the two quantities as indices to study the day to  
346 day variation of ionospheric behaviour in this work.

347 The values of these entropy measures were also computed in order to study the dynamical  
348 complexity of the system under observation (the ionosphere). The day to day values of Tsallis  
349 entropy were computed for the entire year for different stations. The day to day values of Tsallis  
350 entropy plotted for the Enugu station and for Toro station are shown in fig 9(a and b). The plots  
351 of the day to day values show the transient variation of the ionosphere and a wavelike yearly  
352 pattern.

### 353 **3.2 Non linearity Test using surrogate data**

354 The test for non-linearity using the method of surrogate data according to Kantz and Schreiber  
355 (2003) has proven to be a good test for non-linearity in time series describing a system. It has  
356 been accepted that the method of surrogate data test could be a successful tool for the  
357 identification of nonlinear deterministic structure in an experimental data (Pavlos et al., 1999).  
358 This method involves creating a test of significance of difference between linearly developed  
359 surrogate and original nonlinear time series to be tested. The test is done by carrying out the  
360 computation of the same quantity on both surrogates and the original time series and then  
361 checking for the significance of difference between the results obtained from the surrogates with  
362 the original data. Theiler et al (1992) suggested the creation of surrogate data by using Monte  
363 Carlo techniques for accurate results. According to this method, typical characteristic of data  
364 under study are compared with those of stochastic signals (surrogates), which have the same  
365 auto-correlation function and the power spectrum of the original time series. It can be safely  
366 concluded from the test of significance carried out on the surrogate and the original data that, a  
367 stationary linear Gaussian Stochastic model cannot describe the process under study provided  
368 that the behaviour of the original data and the surrogate data are significantly different.


369

370 In this work 10 surrogate data were generated from the original data set. The geometrical and  
371 dynamical characteristics of the original data were then compared to that of the surrogates using  
372 the statistical method of significance of difference which can be defined as

$$374 \quad S = \frac{\alpha_{Surr} - \alpha_{Original}}{\sigma} \quad (13)$$

375

376 Where  $\alpha_{Surr}$  is the mean value of the computed quantity for the surrogate data and  $\alpha_{Original}$  is  
377 the same quantity computed for the original TEC data,  $\sigma$  is the standard deviation of the same  
378 quantity computed for the surrogate data. The significance of difference considered for the null  
379 hypothesis to be rejected here is greater than 2, which enables us to be able to reject the null  
380 hypothesis that the original TEC data describing the ionospheric system can be modeled using a  
381 Gaussian linear stochastic model with confidence greater than 95%.

382 The surrogate data test for all stations used in this study show that the Lyapunov exponent of  
383 the surrogate data for the selected days in October are shown in the Table below The results  
384 show that the surrogate data test for Lyapunov exponent show a significance of difference  
385 greater than 2 for all the selected days for all the stations. Similar results were obtained for  
386 Mutual Information, Fraction of False Nearest Neighbours and Correlation Dimension. This  
387 result gives us the confidence to reject the null hypothesis that the data used cannot be modeled  
388 using a linear Gaussian stochastic model, which shows that the system is a nonlinear system with  
389 some level of determinism. Fig. 10 shows the plots comparing the mutual information plotted  
390 against time delay for the original detrended data blue with the mutual information for the  
391 surrogate data for TEC data measured at Lagos for the quietest day of March 2011, while Fig. 11  
392 is comparing fraction of false nearest neighbours for the same set of data. Tables 2a shows the  
393 values of Lyapunov exponents for both original detrended and its surrogate data for TEC  
394 measured in Lagos during the quietest days and Table 2b shows the values of Lyapunov  
395 exponents for both original detrended and its surrogate data for TEC measured in Lagos during  
396 the most disturbed days of October 2011. 

397

398

### 399 3.3 Trend filtering using the moving average approach for the daily Values

400 The trend of a fluctuating time series can be made clearer to reveal the general pattern of that  
401 time series, and to make the fluctuating pattern of the daily variation of the chaoticity and  
402 dynamical complexity measures clearer in the work, the moving average method has been  
403 employed. The method of moving average filtering has found its applications geophysics (e.g.  
404 Bloomfield 1992; Bloomfield and Nychka 1992; Baillie and Chung 2002), and in other areas like  
405 financial time series analysis, microeconomics, biological sciences and medical sciences. The  
406 various fields mentioned require different trend filtering method depending on the structure of  
407 the time series to be analyzed. Different filtering processes that can be used to reveal the trend  
408 includes the moving average filters, exponential filters, band-pass filtering, median filtering etc.

409 Suppose we have a time series  $z[t]$  such that  $t = 1, 2, 3 \dots \dots n$ , where 'n' could assume any  
410 value. If  $z[t]$  consists of a consistent varying trend component that appears over a longer period  
411 of time  $t$  given as  $u[t]$  and a more rapidly varying component  $v[t]$ . The goal of trend filtering in  
412 any research is to estimate either of the two components (Kim et al., 2009). The purpose of trend  
413 filtering in this work is to further reveal the general slow varying trend that appears to be obvious  
414 in the daily variation of the values of the chaoticity and dynamical complexity of the ionosphere,  
415 which might appear to be obviously varying with the yearly solar activity (a quantity with slow  
416 varying trend). To make  $u[t]$  which represents the general slow varying trend smoother and in  
417 the process reduce  $v[t]$  we apply the moving average filter.

418 If we assume  $z[t]$  to be our time series representing the daily variation of the values of the  
419 chaoticity and dynamical complexity of the ionosphere, then our smoothing with weighting  
420 vector/filter  $w_j$  will create the new sequence  $u_j$  as

$$421 \quad u[t] = z[t] * w[n] = \frac{1}{2k+1} \sum_{i=-k}^k x[n - 1]. \quad (14)$$

422 In this work the Savitzky-Golay method of smoothing proposed by Savitzky and Goley (1967),  
423 which is a generalized form of moving average was applied to the trend smoothing of the daily  
424 variation of the chaoticity and dynamical complexity of the ionosphere. In this case it performs a  
425 least square fit to a small set of  $L(= 2k + 1)$  consecutive data to a polynomial and then takes

426 midpoint of the polynomial curve as output. The smoothed time series in this work will now be  
427 given as

$$428 \quad u[t] = z[t] * \omega[n] = \frac{\sum_{i=-k}^k A_i * x[n-1]}{\sum_{i=-k}^k A_i} \quad (15)$$

429 where,  $\omega[n] = \frac{A_n}{\sum_{i=-k}^k A_i}$ ,  $-k \leq n \leq k$  such that  $A_i$  controls the order of polynomial. A similar  
430 method was described in Reddy et al., (2010).

431 The smoothed daily variation and the original data and the plot of the smoothed variation only,  
432 for the Lyapunov exponents of the detrended TEC measured at the Enugu and Toro are shown in  
433 fig 12(a and b). The smoothed day to day variation for Tsallis entropy for the detrended TEC  
434 measured at Enugu and Toro stations respectively are shown in fig 13(a and b).

435

#### 436 **4.0 DISCUSSION**

437 The results presented in the work reveals the dynamical characteristics of the ionosphere. These  
438 characteristics are being discussed in this section, considering the time series treatment and phase  
439 space reconstruction; the study of chaos using chaotic quantifiers and the use and comparison of  
440 dynamical complexity measures in terms of their response to the variations on ionospheric  
441 dynamics. Also being discussed, is the implication of the nonlinearity test using the surrogate  
442 data and the comparison of the two quantifiers and their viability as indices for the continuous  
443 study and characterization of the ionosphere

444

445 The time series analysis shows the appearance of some degree of nonlinearity in the internal  
446 dynamics of the ionosphere. The time series plot in Fig. 1 shows the rise in TEC to peak at the  
447 sunlit hours of the day, however it can be seen that the rising to the peak exhibited by the  
448 ionosphere, which is the dominant dynamics during the day, make it impossible to clearly see the  
449 internal dynamics of the system from the TEC time series plot. It can be seen that the TEC time  
450 series curve is not a smooth curve with tiny variations, which probably describes a part of the  
451 internal dynamics. These visible tiny variations around the edges of the time series plot can be  
452 regarded as rate of change of TEC which is a phenomenon that can describe the influence of



453 scintillations in the ionosphere these variations are however more obvious during the night time  
454 between 1100th and 1440th minutes of the day (that is, between about 1800 and 2400 hours of  
455 the day). It should be noted here that scintillations has been described as a night time phenomena  
456 associated with spread-F, and it occurs around pre-midnight and post-midnight periods (Vyas  
457 and Chandra 1994; Vyas and Dayanandan 2011; Mukherjee et al.,2012; Bhattacharyya and  
458 Pandit 2014). The detrended data shows the internal dynamics of the system more clearly, with a  
459 pattern similar to the values around night period mentioned earlier. The post-sunset values  
460 (especially at night time) in Fig.1 show a pattern similar pattern with the detrended TEC plot in  
461 Fig 2. It has been established that TEC does not decrease totally throughout the night as expected  
462 normally through simple theory that TEC builds up during the day, but it shows some anomalous  
463 enhancements and variations and this can occur under a wide range of geophysical conditions  
464 (Balan and Rao, 1987; Balan et al., 1991;Unnikrishnan and Ravindran, 2010). The delay  
465 representation of the phase space reconstruction shows a trajectory that is clustered around its  
466 origin, for all the stations, which can be seen as an indication of the possible presence of chaos.  
467 The degree of closeness of these trajectories however varies for different days from one station  
468 to another, resulting from varying degrees of variations in stochasticity and determinism. The  
469 varying degrees of variations in stochasticity and determinism can be attributed to the daily  
470 variations and local time variations of photoionization, recombination, influx of solar wind and  
471 other factors that may influence the daily variations of TEC (Unnikrishnan 2010).

472


473 The positive values of Lyapunov exponent indicate the presence of chaos (Wolf et al., 1985;  
474 Rosenstein et al., 1993; Hegger et al., 1999; Kantz and Schreiber, 2003). The presence of chaos  
475 was revealed by the positive Lyapunov exponent computed from all stations and this as a result  
476 of the fact that the ionosphere is a system controlled by many parameters influencing its internal  
477 dynamics. Because of its extreme sensitivity to solar activity, the ionosphere is a very sensitive  
478 monitor of solar events. The ionospheric structure and peak densities in the ionosphere vary  
479 greatly with time (sunspot cycle, seasonally and diurnally), with geographical location (polar,  
480 auroral zones, mild-latitudes, and equatorial regions), and with certain solar-related ionospheric  
481 disturbances. During and following a geomagnetic storm, the ionospheric changes around the  
482 globe, as observed from ground site can appear chaotic (Fuller-Rowell et al., 1994; Cosolini and  
483 Chang, 2001; Unnikrishnan and Ravindran, 2010). The recorded presence of chaos as indicated

484 by the positive values of Lyapunov exponent was found in all the computations, for all the TEC  
485 values obtained for the selected days from all the measuring stations used in this work. This can  
486 be expected as it agrees with results from previous works that show that there is a reasonable  
487 presence of chaos in the ionosphere, even in the midst of the influence of stochastic drivers like  
488 solar wind (Bhattacharyya, 1990; Wernik and Yeh, 1994; Kumar et al., 2004; Unnikrishnan et  
489 al., 2006a,b; Unnikrishnan, 2010). However the values of Lyapunov exponents vary from day to  
490 day due to variations in ionospheric processes for different days on the same latitude as seen in  
491 Fig. 7(a and b) with Fig. 12(a and b) showing the day to day variation (upper panel) and the  
492 smoothed curve of the day to day variation (lower panel) for the entire year. There are also  
493 latitudinal variations due to spatial variations in the various ionospheric processes taking place  
494 simultaneously. The ionosphere is said to have a complex structure due to these varying  
495 ionospheric processes.

496 The higher values of Lyapunov exponent during months of low solar activity (the solstices) is an  
497 evidence that that the rate of exponential growth in infinitesimal perturbations in the ionosphere  
498 leading to chaotic dynamics might be of higher degree during most of the days of those months  
499 compared to days of the months with high solar activities showing lower values of Lyapunov  
500 exponents (Unnikrishnan 2010, Unnikrishnan and Ravindran, 2010).

501  
502 The results of the correlation dimension values computed are within the range of 2.7 to 3.2 with  
503 the lower values occurring mostly during the storm periods. The lower dimension during the  
504 storm periods compared to the quiet days may be due to the effect of a stochastic drivers like  
505 strong solar wind and solar flares, that occurs during geomagnetic storms on the internal  
506 dynamics of the ionosphere, this could have been as a result of the fact that the internal dynamics  
507 must have been suppressed by the external influence. The restructuring of the internal dynamics  
508 of the ionosphere might be responsible for low dimension chaos during storm and also the lower  
509 values of other measures like the Lyapunov exponents. The relatively disturbed day however  
510 might have a higher dimension so long as it is not a storm period, and sometimes a relatively  
511 disturbed day of the month might be a day with storm and in this case there is usually a lower  
512 value of chaoticity and sometimes lower values of correlation dimension as well. The lower  
513 value of chaoticity and dimension in ionosphere during storms indicates a phase transition from  
514 higher values during the quiet periods to lower values during storm periods which may be due to

515 the modification of the ionosphere by the influx of high intensity solar wind during the storm  
516 period (Unnikrishnan et al., 2006a, b; Unnikrishnan 2010; Unnikrishnan and Ravindran, 2010).

517  
518 The surrogate data test shows significance of difference greater than 2 for all the computed  
519 measures which enables rejection of the null hypothesis that the ionospheric system can be  
520 represented with a linear model for all the data used from the stations. However it was  
521 discovered that the lower significance of difference corresponds to the lower values of Lyapunov  
522 exponents during storm and extremely disturbed periods (see tables 2 and 3). This may be due  
523 the rise in stochasticity during the storm period as a result of drop in values of computed  
524 quantities like Lyapunov exponents. Our ability to reject the Null hypothesis for all stations  
525 however shows the presence of determinism and confirms that the underlying dynamics of the  
526 ionosphere is mostly non-linear. This further validates the presence of chaos since the surrogate  
527 data test for non-linearity show that out detrended TEC is not a Gaussian (linear) stochastic  
528 signal (Unnikrishnan 2010). 

529  
530  
531 The Tsallis entropy was able to show the deterministic behavior of the ionosphere considering  
532 its response during storm periods compared to other relatively quiet periods as the rapid drop in  
533 values of Tsallis entropy during storm show that there is a transition from higher complexity  
534 during quiet period to lower complexity during storms, this response in the values of Tsallis  
535 entropy is similar to the response of Lyapunov exponent values during storm. This reaction to  
536 storm shown by the values of Tsallis entropy computed for TEC was also described by the  
537 reaction of Tsallis entropy computed for Dst during storm periods (Balasis et al., 2008, 2009). A  
538 closer observation of the day-to-day variability within a month shows that the values were much  
539 lower for storm periods compared to the nearest relative quiet period. For example, the storm  
540 that occurred on the 25th of October resulted in lower values of Lyapunov exponent and Tsallis  
541 entropy compared to relatively quiet days close to it. The reaction to storm may be due to the  
542 influence of stochastic driver like strong solar wind flowing into the system as a result of solar  
543 flare or CMEs that produces the geomagnetic storms. Although there is always an influence of  
544 corpuscular radiation in form of solar wind flowing from the sun into the ionosphere, the  
545 influence is usually low for days without storm compared to days with geomagnetic storms as a

546 result of solar flares, CMEs etc (Unnikrishnan et al., 2006a,b; Unnikrishnan, 2010, Ogunsua et al  
547 2014).

548  
549 The presence of chaos and high variations in the dynamical complexity, even at quiet periods in  
550 the ionosphere may be due to the internal dynamics and inherent irregularities of the ionosphere  
551 which exhibit non-linear properties. However, this inherent dynamics may be complicated by  
552 external factors like Geomagnetic storms. This may be the main reason for the drop in the values  
553 of Lyapunov exponent and Tsallis entropy during storms. According to Unnikrishnan et al.,  
554 (2006a,b), geomagnetic storms are extreme forms of space weather, during which external  
555 driving forces , mainly due to solar wind, subsequent plasmasphere -ionosphere coupling, and  
556 related disturbed electric field and wind patterns will develop. This in turn creates many active  
557 degrees of freedom with various levels of coupling among them, which alters and modifies the  
558 quiet time states of ionosphere, during a storm period. This new situation developed by a storm,  
559 may modify the stability/instability conditions of ionosphere, due to the superposition of various  
560 active degrees of freedom.

561  
562 The observation from the day-to-day variability of Lyapunov exponent and Tsallis entropy also  
563 show irregular pattern for all stations. These irregular variations might be due to the same factors  
564 mentioned before (i.e internal irregularities due to so many factors described and also due to  
565 variation in the influx of the external stochastic drivers). The day-to-day variability for the entire  
566 year shows a “wavelike” pattern with the values dropping to lower values during the equinox  
567 months especially during March-April equinox. The wavelike pattern has been found to be  
568 similar for different stations as seen in Figs. 7 & 12 and Figs. 9 & 13 for Lyapunov exponents and  
569 Tsallis entropy respectively. Figs.9 and 13 show the smoothed curves for Lyapunov exponent  
570 and Tsallis entropy respectively, with the drop in values at equinoxes showing more clearly. The  
571 phase transition in chaoticity and dynamical complexity is also responsible for the wavelike  
572 variations, with values of Lyapunov exponent and Tsallis entropy dropping during the equinoxial  
573 months, and this may be due to the influence of the daily influx of the solar wind having higher  
574 values during equinoxes due to the proximity of the Earth to the sun during this period compared  
575 to the solstice months.

576

577 The wavelike pattern observed has been described to be as a result of self organized critical  
578 (SOC) phenomenon, a phenomenon which has been found to exist in both the magnetosphere  
579 and the ionosphere or the space plasma system in general, due to coupling between the two  
580 systems, since the magnetosphere couples the ionosphere tightly to the solar wind (Lui, 2002).  
581 Many literatures has shown the existence of chaos in the SOC in the magnetosphere (chang et  
582 al.,1992,1998,1999; Consolini et al., 1996 Chapman et al., 1998; Freeman and Watkins 2002  
583 and; Koselov and Koselova, 2001. Uritsky et al., (2003) and; Chang et al., (1992). The existence  
584 of SOC in space plasma system involving both the ionosphere the the magnetosphere was  
585 described by (Lui, 2002; Chang et al., 2002; Chang et al., 2004) .

586

587 The variation along the latitude also shows the inconsistence and complexity of the ionospheric  
588 processes. This is the reason why for the same day of the month the values of Lyapunov  
589 exponent vary from one station to another. Lyapunov exponent however, appears to respond  
590 better to changes in solar activities compared to Tsallis entropy with more distinct results. This  
591 may be due to the fact that Tsallis entropy being not only a measure of complexity, but also a  
592 measure of disorderliness in a system might not be as perfect in describing chaos as Lyapunov  
593 exponent. Kalogeropoulos (2009) and Baranger et.al (2002) observed that Tsallis entropy has a  
594 relationship that is not totally linear in all cases at different level of chaos with Lyapunov  
595 exponent as a measure of chaos.

596

597 There are also many variations in the internal dynamics of the ionosphere that could lead to  
598 changes in chaotic behavior. The variations of Lyapunov exponents during quiet days might be  
599 as a result of different variations in the intrinsic dynamics of the ionosphere. Difference in  
600 variation pattern at different stations for the same quiet day might also be due to the same reason.  
601 It can be affirmed that the ionosphere is a complex system that varies with a short latitudinal or  
602 longitudinal interval such that even stations with one or two degrees of latitudinal differences  
603 might record different values on the same day for both quiet and disturbed periods and that the  
604 same might also occur for storm periods. This is illustrated by the different pattern of variation of  
605 TEC recorded from different stations within such a close range as used in this study.

606

607 These Latitudinal variation in the values of Lyapunov exponents and Tsallis entropy can be  
608 further described by the behavior of the TEC because there can be a more sporadic rate of  
609 change in TEC as seen in the time series plots as a result of irregularities in the internal dynamics  
610 of the ionosphere, which might be as a result of plasma bubbles. Irregularities develop in the  
611 evening hours at F region altitudes of magnetic equator, in the form of depletions, frequently  
612 referred to as bubbles. The edges of these depletions are very sharp resulting in large time rate of  
613 TEC in the equatorial ionosphere, even during magnetically quiet conditions. The large gradient  
614 of the equatorial ionization persists in the local post-sunset hours till about 2100 h LT.  
615 (DasGupta et al., 2007; Unnikrishnan and Ravindran, 2010). The TEC data for one station might  
616 experience an extremely sharp rate of change in TEC that may be due to some plasma bubbles in  
617 that region while the TEC from the other station stays normal. These variations in the various  
618 internal dynamics like plasma bubbles leading to scintillation can cause variations in the  
619 dynamical response of the TEC. Hence, the irregular variation in the values of the Lyapunov  
620 exponent and Tsallis entropy even in quiet periods for two relatively close stations may be due to  
621 these irregularities. This might also be responsible for the quiet days in the same station having  
622 lower values of Lyapunov exponent compared to higher values recorded for disturbed days  
623 without the external influence of storms.

624  
625 The variations of these chaos and dynamical complexity parameters might also be as a result of  
626 the anomalous TEC enhancements that might occur at nights (Balan and Rao (1987); Balan et  
627 al., 1991). These effects can also be seen more clearly in the Tsallis entropy values for the five  
628 period window for quiet day of January, 2011, because the night time value is higher and it also  
629 show a much higher series of fluctuations during this period compared to other periods. As  
630 mentioned in Unnikrishnan and Ravindran (2010), the irregular changes in the dynamical  
631 characteristics of TEC from the results of Lyapunov exponent and Tsallis entropy also may be  
632 due to the collisional Raleigh-Taylor instability which may give rise to a few large irregularities  
633 in L band measurements (Rama Rao et al., 2006; Sripathi et al., 2008) all these can be seen as  
634 internal factors responsible for variations in the dynamical response of TEC as recorded from the  
635 values of the Lyapunov exponents and Tsallis entropy completed for days without storm which  
636 might be quiet or disturbed according to classification and also could account for higher values

637 of these qualifiers during disturbed days compared quiet days. During storms however, the  
638 values were much lower

639  
640 Earlier we, (Ogunsua et al., 2014) showed the appearance and variation of chaoticity quiet and  
641 disturbed day classification by international most quiet day (IQD) and internal most disturbed  
642 day (IDD) classification, as compared to quiet and storm period used by Unnikrishnan (2006;  
643 2010). We were able establish that a relatively quiet day may be less chaotic compared to a  
644 relatively disturbed day unlike the result presented by Unnikrishnan (2006; 2010) for quiet and  
645 storm period. Also the combined use of both Lyapunov exponent and Tsallis entropy for the first  
646 time was found to have a high correlation mostly above 80%, which has stimulated the interest  
647 for further research using the two diagnosis for the study of ionospheric dynamics.

648  
649 This work on the other hand presents the results for day to day variation and has revealed a  
650 seasonal trend for both Lyapunov exponents and Tsallis entropy, which appear in wavelike in  
651 form, with troughs during the two equinoxes. This was established for different stations used in  
652 this research work. The results show the appearance of seasonal trend in spite of the sporadic  
653 daily variation resulting from various changes in the internal dynamics. The seasonal trend has  
654 provided another possible evidence of higher energy input during equinoxes, since it reveals the  
655 effect of the annual energy input to the ionosphere. The day to day response these parameters has  
656 also revealed the variations in the underlying dynamics of the system.

657  
658 As a similarity between the present work and Ogunsua et al. (2014) the relationship between  
659 Lyapunov exponent and Tsallis entropy can also be seen from this work, as the two quantifiers  
660 exhibit similarities in their response to the dynamical behavior of the ionosphere with phase  
661 transition at the same periods of time for all stations. A further investigation of this relationship  
662 shows that all the daily values of Tsallis entropy correlates positively with the values of  
663 Lyapunov exponent at values between 0.78 and 0.83.

664  
665 The ability of these quantifiers to clearly reveal the ionospheric dynamical response to solar  
666 activities and changes in its internal dynamics due to other factors is a valid proof of the

667 authenticity of the use of these chaotic and dynamical measures, as indices for ionospheric  
668 studies.

669

## 670 **5.0 Conclusion**

671 The chaotic behaviour and dynamical complexity of low latitude ionosphere over some parts of  
672 Nigeria was investigated using TEC time series measured Simultaneously at five different  
673 stations namely Birnin Kebbi (geographic coordinates  $12^{\circ}32'N$ ,  $4^{\circ}12'E$  ; dip latitude  $0.62^{\circ}N$ ),  
674 Torro (geographic coordinates  $10^{\circ}03'N$ ,  $9^{\circ}04'E$  ; dip latitude  $-0.82^{\circ}N$ ), Enugu (geographic  
675 coordinates  $6^{\circ}26'N$ ,  $7^{\circ}30'E$  ; dip latitude  $-3.21^{\circ}N$ ), Lagos (geographic coordinates  $6^{\circ}27'N$ ,  
676  $3^{\circ}23'E$  ; dip latitude  $-3.07^{\circ}N$ ) and Yola (geographic coordinates  $9^{\circ}12'N$ ,  $12^{\circ}30'E$  ; dip  
677 latitude  $-1.39^{\circ}N$ ) within the low latitude region. The detrended TEC time series data obtained  
678 from the GPS data measurement were studied for chaoticity using phase space reconstruction  
679 techniques, computation of Lyapunov exponents and correlation dimension. Tsallis entropy was  
680 used for the study of dynamical complexity of the ionospheric system described by the TEC data.

681 The detrended TEC time series were subjected to further analysis for phase space reconstruction  
682 from which the choice of time delay of 30 was obtained and an embedding dimension of 5 were  
683 considered in this study. The evidence of the presence of chaos in all the time series data was  
684 obtained for all the data used, as indicated by the positive Lyapunov exponent. The results of  
685 Tsallis entropy show the variations in the dynamical complexity of the ionosphere, which may be  
686 due to geomagnetic storms and other phenomena like changes in the internal irregularities of the  
687 ionosphere. The response of the Tsallis entropy to various changes in the ionosphere also shows  
688 the deterministic nature of the system. The results of the Tsallis entropy show a lot of similarities  
689 with that of the Lyapunov exponents, with both results showing a phase transition from higher  
690 values in the solstices to lower values during the equinoxial months. The values of Lyapunov  
691 exponent were found lower for the days of the months in which storm was recorded relative to  
692 the nearest relatively quiet days which agree with previous works by other investigators. A  
693 similar pattern of results was obtained for the computed values of Tsallis entropy. The random  
694 variations in the values of chaoticity in the detrended TEC describing the internal dynamics of  
695 the ionosphere as seen in the result obtained from both Lyapunov exponent and Tsallis entropy  
696 depicts the ionosphere as a system with a continuously changing internal dynamics, which shows



697 that the ionosphere is not totally deterministic but also has some elements of stochasticity  
698 influencing its dynamical behaviour.


699

700 The phase transition in the systems of the ionosphere resulting in the lower values of the  
701 chaoticity and dynamical complexity quantifiers during the geomagnetic storms and the  
702 equinoxial months is the evidence that the ionosphere can be greatly modified by stochastic  
703 drivers like solar wind and other incoming particle systems. It can also be seen that the results  
704 of Tsallis entropy follow the same pattern with Lyapunov exponent, which shows show that both  
705 can be use simultaneously and comparatively as measures of chaos and dynamical complexity as  
706 the correlation of all the values obtained for both quantities give values between 0.78 and 0.81.

707

708 Although the knowledge of being able to characterize the ionospheric behaviour using the two m  
709 ajor quantifiers shows their ability to measure level of determinism when used together, the relat  
710 ionship between these two quantifiers calls for more research, in the use of these qualifiers, to en  
711 able proper description and characterization of the state of ionosphere. The response of both Tsal  
712 lis entropy and Lyapunov exponents to changes in the ionosphere shows that the two quantifiers  
713 can be used as indices to describe the processes/dynamics of the ionosphere.

714

715 Even though we cannot conclude totally until further investigations have been carried out on vari  
716 ous properties of the ionosphere describing its dynamics. It can be safely established that this stu  
717 dy has created roadmap for the use of the chaoticity and dynamical complexity measures as indic  
718 es to describe the process/dynamics of the ionosphere. 

719

720

721

722

723

724 **Acknowledgement**

725 The authors appreciate the editorial team and the referees for their contributions which have led  
726 to the final shape of this paper. The GPS data used for this research were obtained from the public  
727 archives of the Office of the Surveyor General of the Federation (OSGoF) of the Federal  
728 Government of Nigeria, which is the mapping agency of Nigeria.

729

730

731

732

733

734

735

736

737

738

739

740

741

742

743

744

745

746 **References**

- 747 Abdu M.A.: Major Phenomena of the equatorial ionosphere thermosphere system under  
748 disturbed conditions, *J.Atmos.Solten Physics.*,59(13), 1505 – 1519, 1997.
- 749 Anastasiadis, A.; Costa, L.; Gonzáles, C.; Honey, C.; Széliga, M. & Terhesiu, D. "Measures of  
750 Structural Complexity in Networks", *Complex Systems Summer School 2005, Santa Fe. (2005).*
- 751 Bak, P., C. Tang, and K. Wiesenfeld, Self-Organized Criticality-an Explanation of 1/F Noise,  
752 *Phys. Rev. Lett.*, 59(4), 381– 384, 1987.
- 753 Balan N., Rao,P.B.: Latitudinal variations of nighttime enhancements in total electron content,  
754 *journal of Geophysical Research* 92 (A4), 3436 – 3440. 1987
- 755 Balan N., Bailey G.J., Balachandian. Nouv R.: Solar and Magnetic effects on the latitudinal  
756 variations of nighttime TEC enhancement, *Annales Geophysicae* 9, 60 – 69. 1991
- 757 Balasis, G., and Manda M.: Can electromagnetic disturbances related to the recent great  
758 earthquakes be detected by satellite magnetometers? *Tectonophysis* – 431, doi:  
759 10.1016/j.texto.2006.05.038. 2007
- 760 Balasis, G., Daglis I.A., Papadimitrou, C., Kalimeri, M., Anastasiadis, A., Eftaxias, K.:  
761 Dynamical complexity in  $D_{st}$  time series using non-extensive Tsallis entropy. *Geophysical*  
762 *Research Letters* 35, L14102, doi:10.1029/2008GL034743. 2008
- 763 Balasis, G., Daglis I.A., Papadimitrou, C., Kalimeri, M., Anastasiadis, A., Eftaxias, K.:  
764 Investigating Dynamical complexity in the magnetosphere using various entropy measures.  
765 *Journal of Geophysical Research* 114, A00D06, doi:10.1029/2008JA014035. 2009
- 766 Ballie R. Chung S.: Modeling and forecasting from trend stationary long memory models, with  
767 applications in climatology. *International journal of forecasting*, 18(2)215-226,2002.
- 768 Bhattacharyya, A: Chaotic behavior of ionosphere turbulence from scintillation measurements, *J.*  
769 *Geophys. Res*, 17, 733 – 738, 1990.

770 Bhattacharyya, A and Pandit J.: Seasonal variation of spread-F occurrence probability at low  
771 latitude and its relation with sunspot number. *International Journal of Electronics and*  
772 *Communication technology* vol 5(2) pp. 40-43. 2014.

773 Bloomfield P.: Trends in global Temperature. *Climate Change*, 21:1-16,1992

774 Bloomfield P. and Nychka D.: Climate spectra and detecting climate change. *Climate Change*,  
775 21:275-287,1992

776 Boon J., and C.Tsallis (Eds.): Nonextensive statistical mechanics: New trends, new  
777 perspectives, *Europhys.Newss*, 36(6), 185 – 231. 2005

778 Burgula,L.F., A.F –Vixas, and C.Wang , Tsallis distribution of magnetic field strength variations  
779 in the heliosphere: 5 to 90 AU, *J. Geophys. Res*, 112, A07206, doi: 10.1029/2006  
780 JA012213.2007

781 Chang, T., Low-Dimensional Behavior and Symmetry-Breaking of Stochastic-Systems Near  
782 Criticality-Can These Effects Be Observed in Space and in the Laboratory, *IEEE Trans. On*  
783 *Plasma Sci.*, 20(6), 691– 694, 1992.

784 Chang, T.: Sporadic localized reconnection and multiscale intermittent turbulence in the  
785 magnetotail, *AGU Monograph No. 104, Geospace Mass and Energy Flow*, (Eds) Horwitz, J. L.,  
786 Gallagher, D. L., and Peterson, W. K., p. 193, (American Geophysical Union, Washington, D.  
787 C.), 1998

788 Chang, T., Self-organized criticality, multi-fractal spectra, sporadic localized reconnections and  
789 intermittent turbulence in the magnetotail, *Phys. of Plasmas*, 6(11), 4137–4145, 1999.

790

791 Chapman, S. C., Watkins, N. W., Dendy, R. O., Helander, P., and Rowlands, G.: A simple  
792 avalanche model as an analogue for magnetospheric activity, *Geophys. Res. Lett.*, 25, 2397–  
793 2400, 1998.

794 Coco I., Consolini, G., Amata, E., Marcucci, M.F., Ambrosino.: Dynamical changes in polar cap  
795 potential structure: an information theory approach. *Nonlinear processes in geophysics.*, 18, 697-  
796 707, 2011.

797 Consolini, G., Marcucci, M. F., and Candidi, M.: Multifractal structure of auroral electrojet index  
798 data, *Phys. Rev. Lett.*, 76 (21), 4082–4085, 1996.

799 Coraddu, M.; Lissia, M.; Tonelli, R. Statistical descriptions of nonlinear systems at the onset of  
800 chaos arXiv:cond-mat/0511736v1 30 Nov 2005 2005

801 Cosolini, G., Chang, T.: Magnetic field topology and criticality in geotail dynamics relevance to  
802 substorm phenomena. *Space Science Reviews* 95, 309-321, 2001.

803 DasGupta, A., Das, A.: Ionospheric total electron content (TEC) studies with GPS in the  
804 equatorial region, *India journal of Radio and space Physics* 36,278-292.2007.

805 Fraser A.M. and Swinney H.L.: independent coordinates for storage attractors from mutual  
806 information, *Phys.Rev,A*, 33, 1134 – 1141, 1986.

807 Freeman, M. P., and N. W. Watkins, The heavens in a pile of sand, *Science*, 298, 979– 980, (1  
808 November ), 2002.

809 Fuller- Rowell, T.J., Codrescu, M.V., Moffett, R.J. Quegan, S.: Response of the magnetosphere  
810 and ionosphere to geomagnetic storms. *Journal of geophysical Research* 99, 3893-3914, 1994.

811 Hegger R., Kantz, H., Shreiber, T.: Practical implementation of nonlinear time series method. The  
812 Tisean package, *Chaos*.9, 413 – 430. 1994

813 Kantz, H. and Shreiber, T.: *Nonlinear time series analysis*. Cambridge university press pp. 69-70,  
814 2<sup>nd</sup> Ed. 2003.

815 Kazimirovsky, E.S. and Vergasova, G.V., *Mesospheric, Lower Thermospheric Dynamics and*  
816 *External Forcing Effects: A Review*, *Indian J. Radio Space Phys.*, vol. 38, no. 1, pp. 7–36, 2009.

817 Kazimirovsky, E.S., Kokourov, V.D., and Vergasova, G.V., *Dynamical Climatology of the*  
818 *Upper Mesosphere, Lower Thermosphere and Ionosphere*, *Surv. Geophys.*, vol. 27, pp. 211–255,  
819 2006.

820 Kennel, M.B., Brown, R., and Abarbanel, H.D.I.: Determining minimum embedding dimension  
821 using a geometrical construction, *Phys. Rev. A*, 45, 3403 – 3411, 1992.

822 Kim S, Koh, K., Boyd S., and Gorivesky D.:  $L_1$  Trend filtering. *SIAM Review*, 51(2):339-360,  
823 2009.

824 Klobuchar, J.: Design and characteristics of the GPS ionospheric time-delay algorithm for single  
825 frequency users, in: Proceedings of PLANS'86 – Position Location and Navigation Symposium,  
826 Las Vegas, Nevada, 280–286, 4–7 November 1986.

827 Kozelov, B. V. and Kozelova, T. V.: Sandpile model analogy of the magnetosphere-ionosphere  
828 substorm activity, Proc. Interball Meeting, Warsaw, Poland, 2001.

829

830 Kumar, K.S., Kumar, C.V.A., George, B., Renuka, G., and Venugopal, C.: Analysis of the  
831 fluctuations of the total electron content, measured at Goose Bay using tools of nonlinear  
832 methods, *J. Geophys. Res.*, 10, A02308, doi: 10.1029/2002/A009768, 2004.

833 Lui. A.T.Y.: Evaluation on the analogy between the dynamic magnetosphere and a forced and/or  
834 self-organised critical system. *Nonlin. Process in Geophys.* 9: 399-407, 2002.

835 Mukherjee, S., Shivalika, S., Purohit, P. K., and Gwal, A. K.: Study of GPS ionospheric  
836 scintillations over equatorial anomaly station Bhopal. *International Journal of Advances in Earth  
837 Science*. Vol 1 (2). Pp. 39-48, 2002.

838 Ogunsua B. O., Laoye J. A., Fuwape I. A., Rabiou A. B.: The comparative study of chaoticity and  
839 dynamical complexity in the equatorial/ low latitude region of the ionosphere over Nigeria  
840 during quiet and disturbed days. *Nonlin process in Geophys* vol. 21, 127-142, 2014.

841 Pavlos, G.P., Kyriakov, G.A., Rigas, A.G., Liatsis, P.I., Trochoulos, P.C., and Tsonis, A.A.:  
842 Evidence for strange attractor structures in space plasma, *Ann. Geophys.*, 10, 309 – 315, 1992,  
843 <http://www.ann-geophys.net/10/309/1992/>

844 Perreault, P. and Akasofu, S.-I.: A study of geomagnetic storms, *Geophys. J. R. Astron. Soc.*, 54,  
845 547–573, 1978.

846 Rabiou, A. B., Mamukuyomi, A. I., Joshua, E. O.: Variability of equatorial ionosphere inferred  
847 from geomagnetic field measurement, Bull. Astro Soc. India. 35, 607-615. India. 2007

848 Rama Rao, P.V.S., Gopi Krishna, S., Niranjan, K., and Prasad, D.S.V.V.D.: Temporal and  
849 Spatial variations in TEC using simultaneous measurements from the india GPS network of  
850 receivers during the low solar activity period of 2004/2005, Ann. Geophys., 24; 3279 – 3292,  
851 doi: 10.5194/angeo -24-3279-2006,2006.

852 Reddy D. S., Reddy N. G., Radhadevi P. V., Saibaba J., and Varadan G.: Peakwise smoothing of  
853 data models using wavelets. *World Academy of Science, Engineering and Technology*, Vol:4  
854 2010 03-24.

855 Remya, R., Unnikrishnan, K.: Chaotic Behaviour of interplanetary magnetic field under various  
856 geomagnetic conditions. *Journal of atmospheric and solar terrestrial Physics*, 72, 662-675, 2010.

857 Rosenstein, M.T., Collins, J.J., DeLuca, C.J.: A practical method for calculation Largest  
858 Lyapunov Exponents from small Data sets. *Physica D*. 65, 117, 1993.

859 Saito, A., Fukao, S., Mayazaki, S.: High resolution mapping of TEC perturbations with the GSI  
860 GPS network over Japan. *Geophysical research letters*, 25, 3079-3082, 1998.

861 Savitzky A., Golay MJE, Smoothing and differentiation by simplified least square procedures.  
862 *Analytical Chemistry* 1964, 36:1627-1639.

863 Shan, H., Hansen, P., Goertz, C. K., and Smith, K. A.: Chaotic appearance of the ae index, *J.*  
864 *Geophys Res.*, 18(2), 147–150, 1991.

865

866 Sindelarova T., Buresova and D., Chum J.: Observations of acoustic-gravity waves in the  
867 ionosphere generated by severe tropospheric weather. *Studia Geophysica et Geodaetica*, Volume  
868 53, Issue 3, pp 403-418 2009. DOI:10.1007/s11200-009-0028-4

869

870 Tsallis, C: Possible generalization of Boltzmann \_Gibbs statistics *J.Stat.phys.*, 52, 487-497. 1988

871 Tsallis,C: Generalised entropy-based criterion for consistent testing. Phys.Rev.E., 58, 1442 –  
872 1445. 1998

873 Tsallis, C: Nonextensive statistics: theoretical, experimental and computational evidences and  
874 connections. *Braz. J. Phys.* [online]. vol.29, n.1, pp. 1-35. ISSN 0103-9733 1999.

875 Unnikrishnan K.,Saito,A., and Fukao,S.: Differences in magnetic storm and quiet ionospheric  
876 deterministic chaotic behavior. GPS TEC Analyses,J. Geophys Res,111, A06304, doi:  
877 10.1029/2005 JA011311, 2006a

878 Unnikrishnan, K., Saito, A., and Fukao, S.: Differences in day and night time ionosphere  
879 determine chaotic behavior : GPS TEC Analyses, J. Geophys. Res, 111, A07310, doi:  
880 10.1029/2005 JA011313, 2006b.

881 Unnikrishnan, K.: comparison of chaotic aspects of magnetosphere under various physical  
882 conditions using AE index time series *Ann. Geophysicae.*, 26, 941-953, 2008.

883 Unnikrishnan, K. Ravindran, S.: A study on chaotic behavior of equatorial/ low latitude  
884 ionosphere over indian subcontinent, using Gps –TEC time series, *J. Atmo. Sol,-Ter. Phy.*, 72,  
885 1080 – 1089, 2010.

886 Unnikrishnan, K.: Comparative study of chaoticity of Equatorial/low latitude ionosphere over  
887 Indian subcontinent during geomagnetically quiet and disturbed periods. *Non Linear Processes in*  
888 *Geophys*, 26, 941-953, 2010.

889

890 Uritsky, V. M., Klimas A. J., and Vassiliadis D.,: Evaluation of spreading critical exponents  
891 from the spatiotemporal evolution of emission regions in the nighttime aurora, *Geophys. Res.*  
892 *Lett.*, 30(15), 1813, doi:10.1029/2002GL016556, 2003.

893

894 Vassiliadis, D.V., Sharma, A.S, Eastman, T.E., and Papadopoulos,K.: Low –dimensionless chaos  
895 in magnetospheric activity from AE time series, *Geophys, Res, let.*, 17, 1841 – 1844, 1990.



896 Vyas, R. M., and Dayanandan B.: Night time VHF ionospheric scintillation characteristics near  
897 crest of Appleton anomaly stations, Udaipur ( $26^{\circ}N$   $73^{\circ}E$ ). Indian Journal of Radio and Space  
898 physics. Vol 40 (4) pp. 191-202, 2011.

899 Vyas, G. D., and Chandra, H.: VHF scintillations and spread-F in the anomaly crest region.  
900 Indian Journal of Radio and Space physics. Vol 23 pp. 157-164, 1994.

901 Wernik, A.W. and Yeh,K.C: Chaotic behavior of ionospheric scintillation modelling and  
902 observations, Radio Sci., 29, 135 – 139, 1994.

903 Wolf, A., Swift,J.B, Swinney, H.L, and Vastano,J.A. : Determining Lyapunov exponents from a  
904 time series, Physica D, 16, 285 – 317, doi: 10.1016/0167 -2789 (85) – 90011-9, 1985.

905

906

907

908

909

910

911

912

913

914

915

916

917

918

919 Table 1: Coordinates of the GPS stations

Station Name	Geographic Coordinates		Dip latitude ( $^{\circ}N$ )
	Long ( $^{\circ}E$ )	Lat( $^{\circ}N$ )	
Birnin Kebbi	$4^{\circ} 12' E$	$12^{\circ} 32' N$	$0.62^{\circ} N$
Torro	$9^{\circ} 04' E$	$10^{\circ} 03' N$	$-0.82^{\circ} N$
Yola	$12^{\circ} 30' E$	$9^{\circ} 12' N$	$-1.39^{\circ} N$
Lagos	$3^{\circ} 23' E$	$6^{\circ} 27' N$	$-3.07^{\circ} N$
Enugu	$7^{\circ} 30' E$	$6^{\circ} 26' N$	$-3.21^{\circ} N$

925

926 Table 2a : Results of Surrogate data test for Lyapunov exponent for TEC data for the quietest  
 927 days of October 2011 at Birnin Kebbi station.

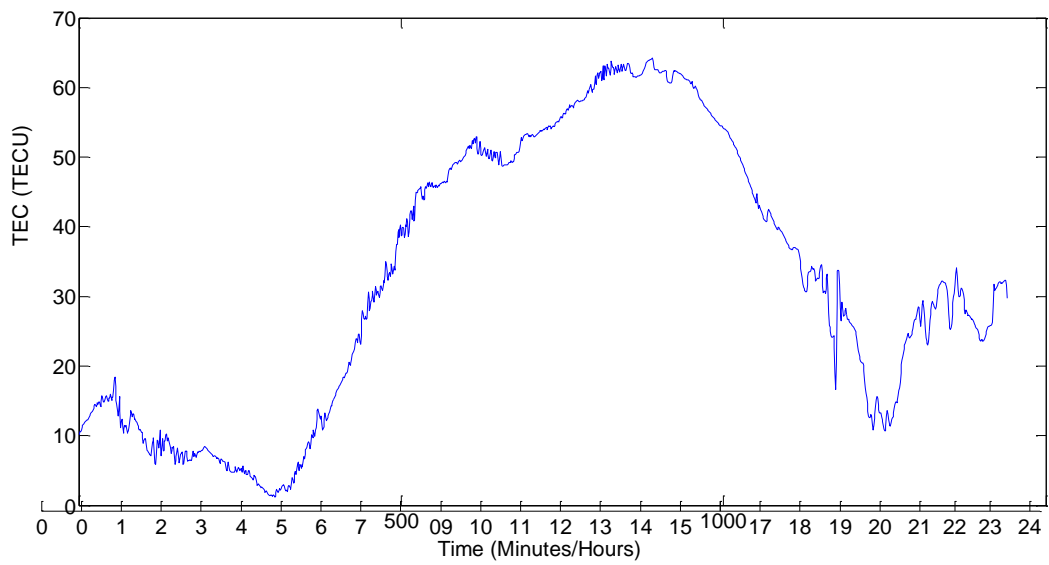
Original Data	Surrogate data
<i>0.1165</i>	<i>0.3921 ± 0.0420</i>
<i>0.0931</i>	<i>0.2029 ± 0.0756</i>
<i>0.1041</i>	<i>0.3860 ± 0.0741</i>
<i>0.0498</i>	<i>0.2891 ± 0.0598</i>
<i>0.1420.</i>	<i>0.3621 ± 0.0504</i>

928

929 Table 2b: Results of Surrogate data test for Lyapunov exponent for TEC data for the most  
 930 disturbed days of October 2011 at Birnin Kebbi station.

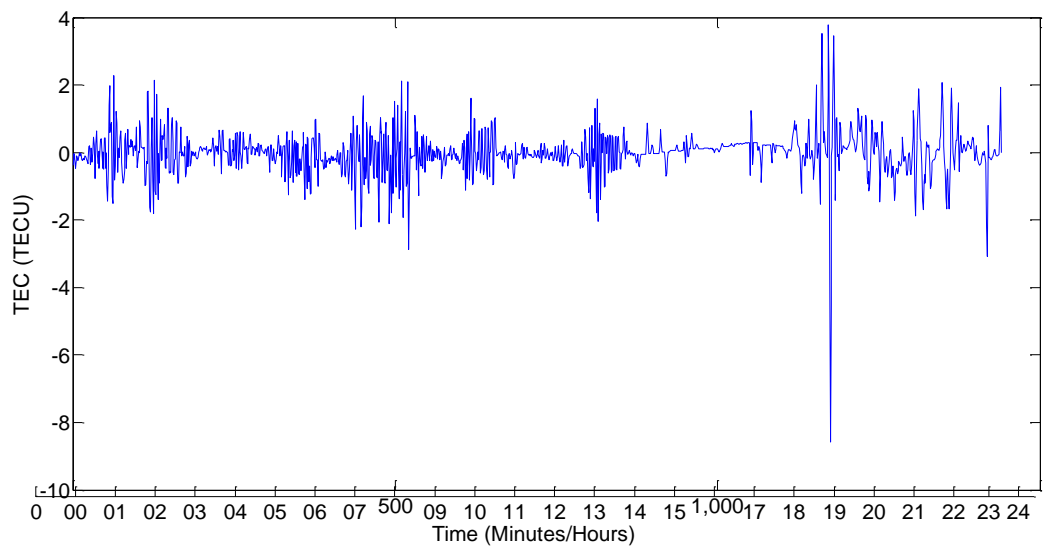
Original Data	Surrogate data
<i>0.0579</i>	<i>0.3039 ± 0.0541</i>
<i>0.0502</i>	<i>0.3156 ± 0.0428</i>
<i>0.0786</i>	<i>0.2527 ± 0.0296</i>
<i>0.1795</i>	<i>0.3662 ± 0.0468</i>
<i>0.1038</i>	<i>0.3100 ± 0.0416</i>

936



937

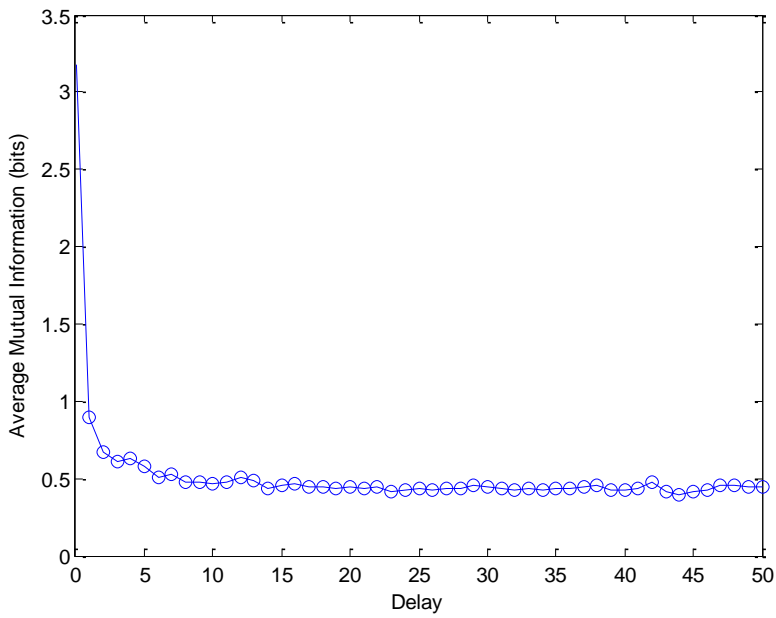
938 Fig 1. A typical time series plot for TEC measured at Lagos for 20 November 2011



939

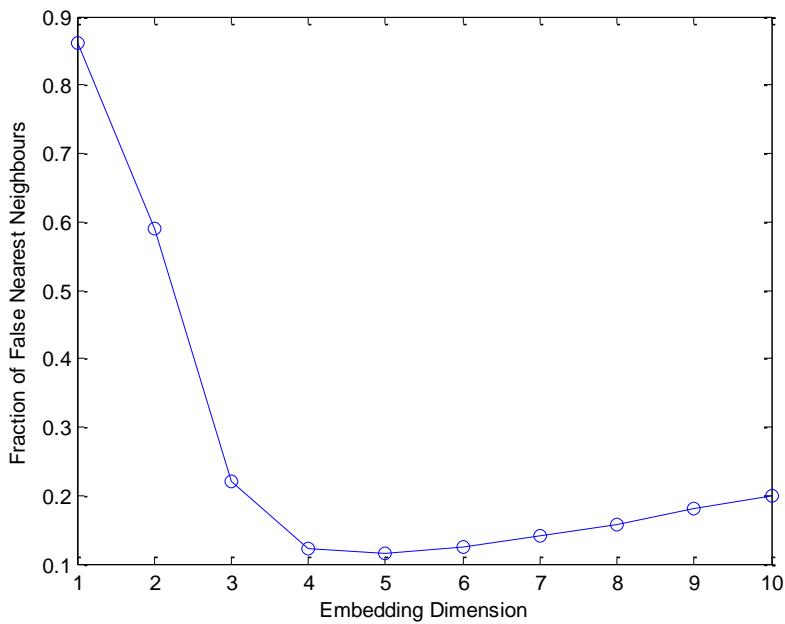
940 Fig 2. The detrended time series plot for TEC measured at Lagos

941



942

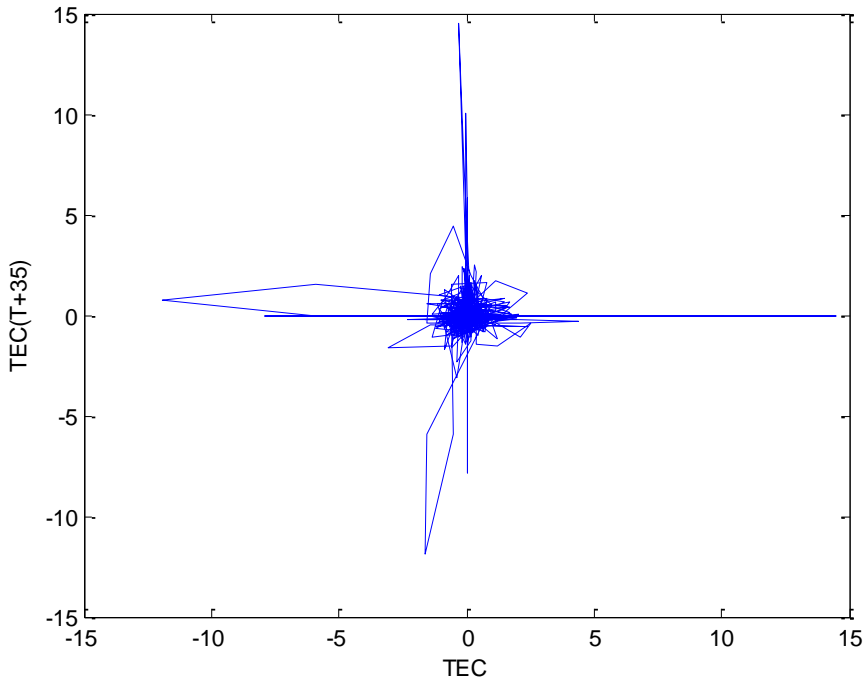
943 Fig. 3 Average mutual information against time Delay for TEC measured at Yola



944

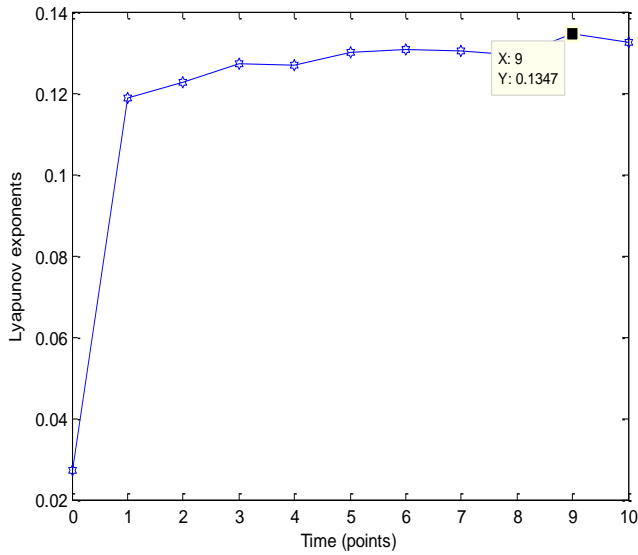
945 Fig. 4 Fraction of false nearest neighbours against embedding dimension for TEC measured at  
 946 yola

947



948

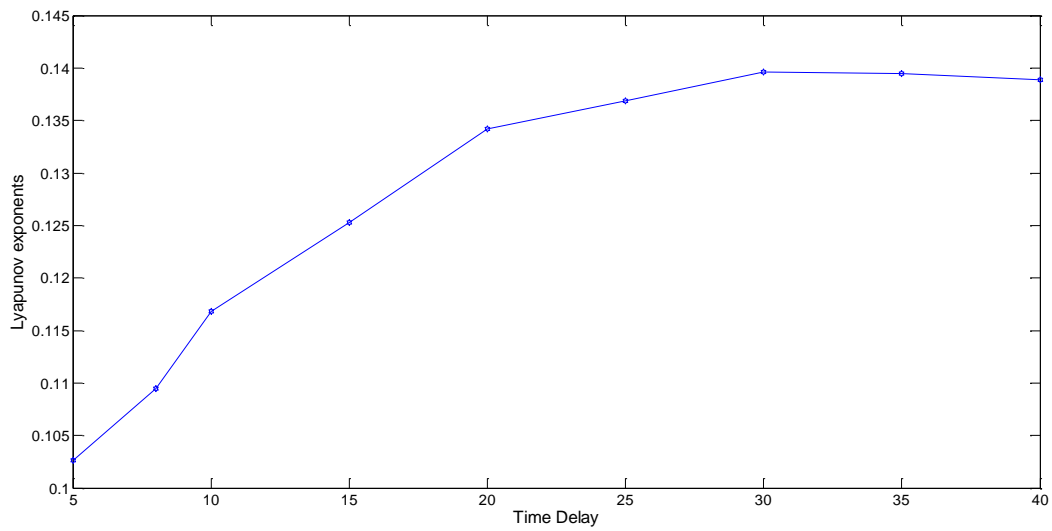
949 Fig.5 The Delay representation of the phase space reconstruction of the detrended TEC



950

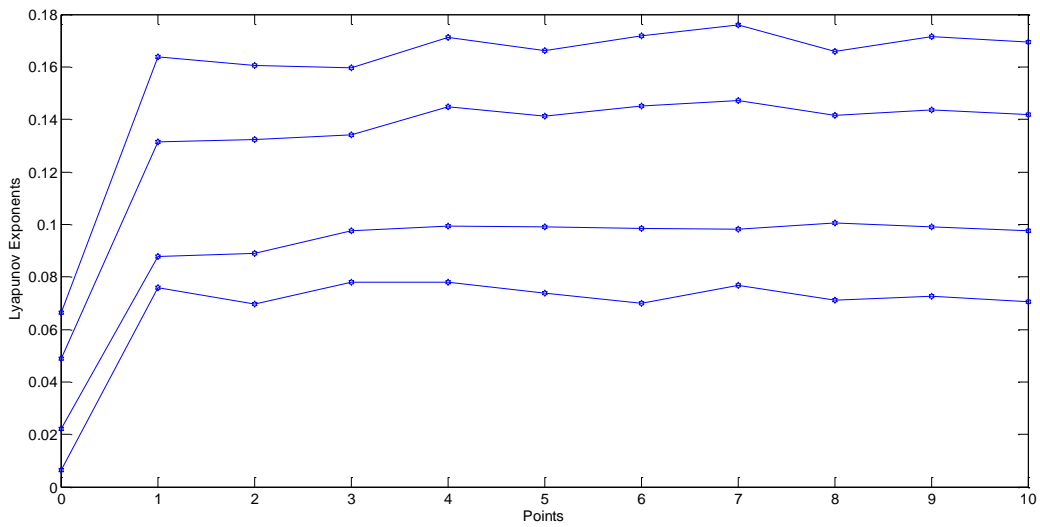
951 Fig. 6 Lyapunov Exponent computed and its evolution, computed as the state space trajectory  
 952 scanned with  $\tau=30$ ,  $m=5$  for detrended time series measured at Yola with Largest Lyapunov  
 953 Exponent equal to 0.1347.

954



955

956 Fig. 6b Lyapunov exponent computed for different time delay with a constant embedding  
957 dimension.



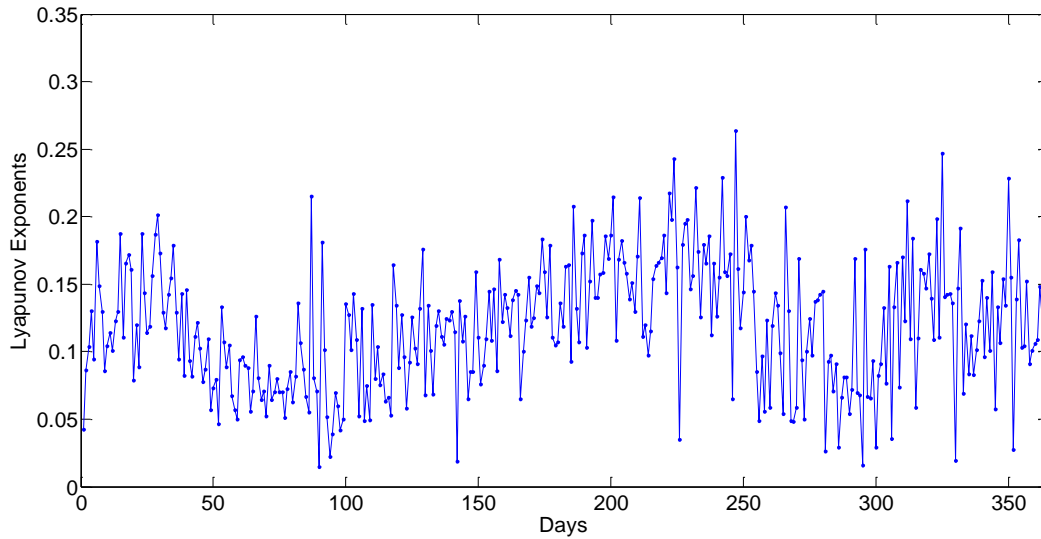
958

959 Fig. 6c Lyapunov exponents computed for different embedding dimension at constant time delay

960

961

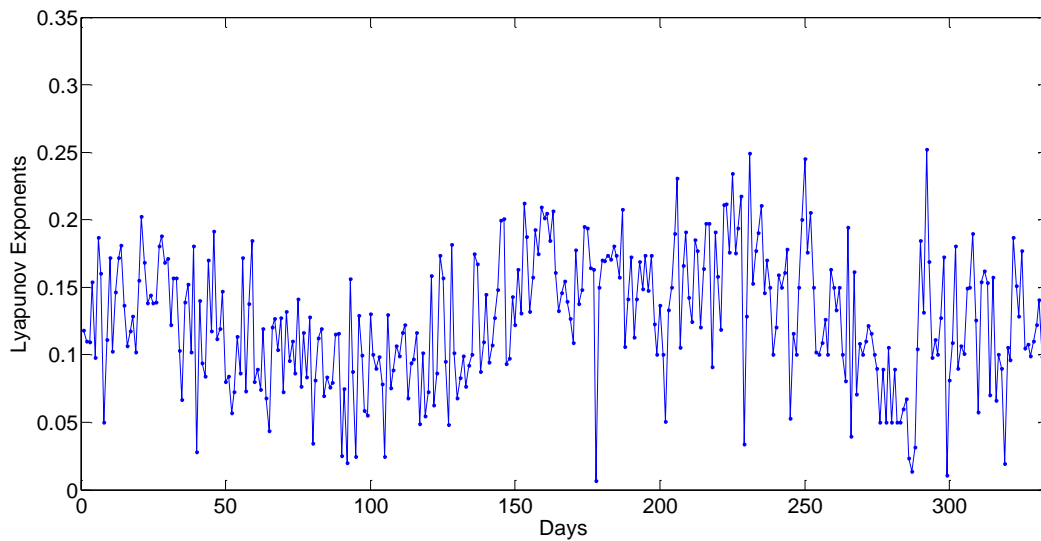
962



963

964 Fig. 7a The transient variations of Lyapunov exponents for 365 days of 2011 for detrended TEC  
965 measured at Enugu

966

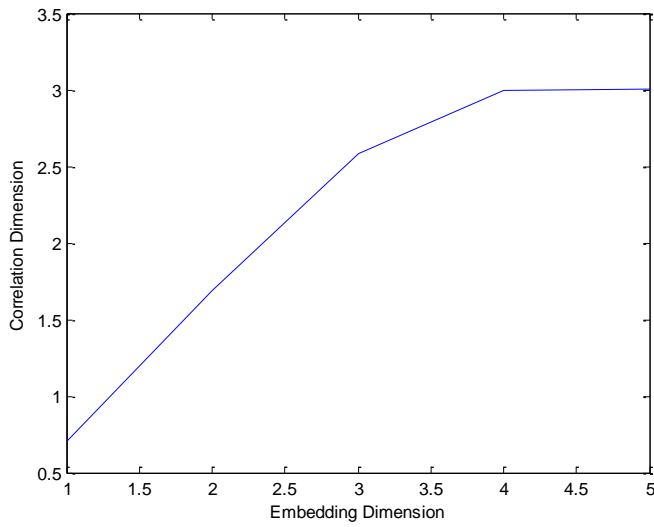


967

968 Fig. 7b The transient variations of Lyapunov exponents for 334 days (Jan 1 –Nov30) of 2011 for  
969 detrended TEC measured at Toro

970

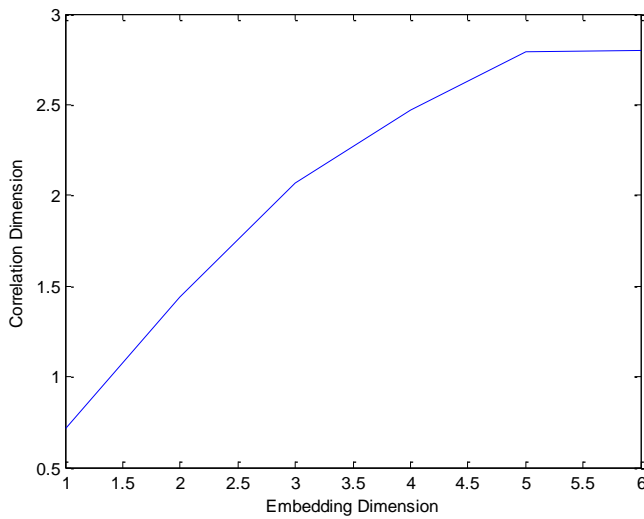
971



972

973 Fig. 8a The correlation dimension of the detrended TEC for the quietest day of October at Birnin  
974 Kebbi which saturates at  $m \geq 4$  and  $\tau = 39$

975



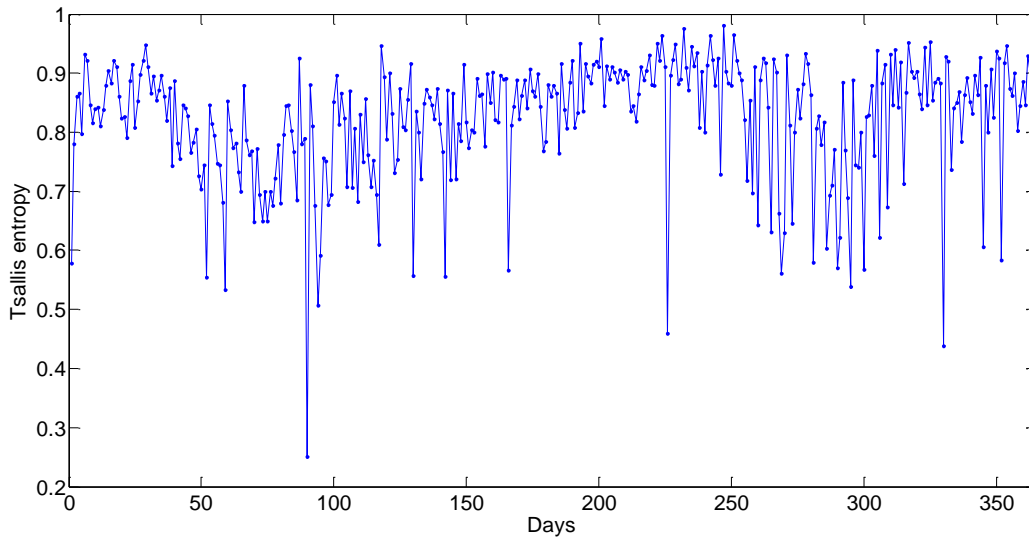
976

977

978 Fig. 8b The correlation dimension of the detrended for the most disturbed day of October at  
979 Birnin Kebbi which saturates at  $m \geq 5$  and  $\tau = 34$

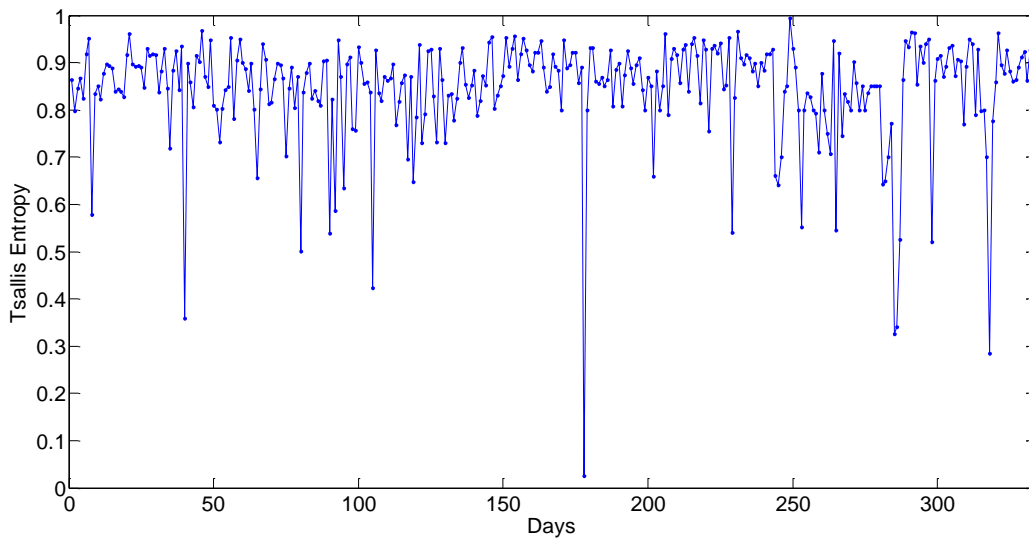


980



981

982 Fig. 9a The transient variations of Tsallis Entropy for 365 days (Jan1 –Nov30) of 2011 for  
983 detrended TEC measured at Enugu

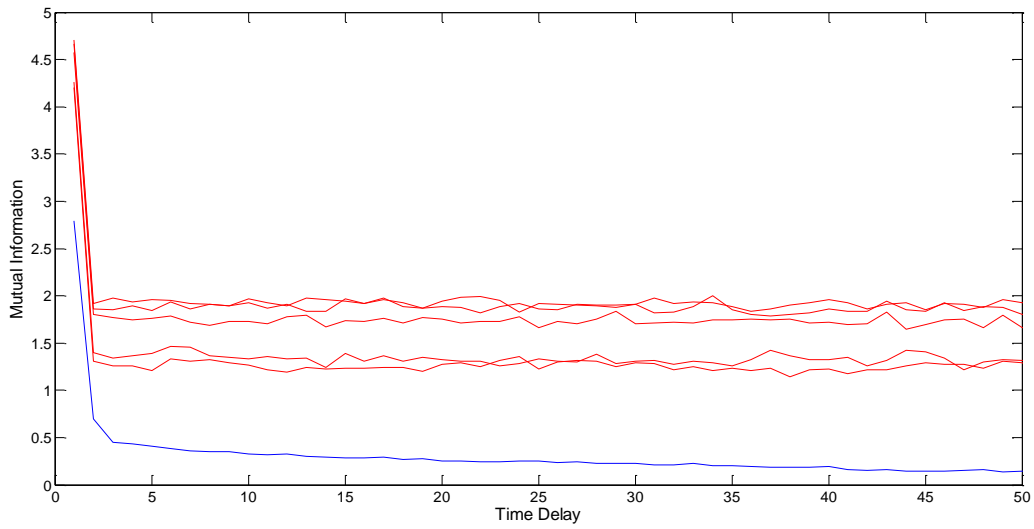


984

985 Fig. 9b The transient variations of Tsallis Entropy for 334 days (Jan1 –Nov30) of 2011 for  
986 detrended TEC measured at Toro

987

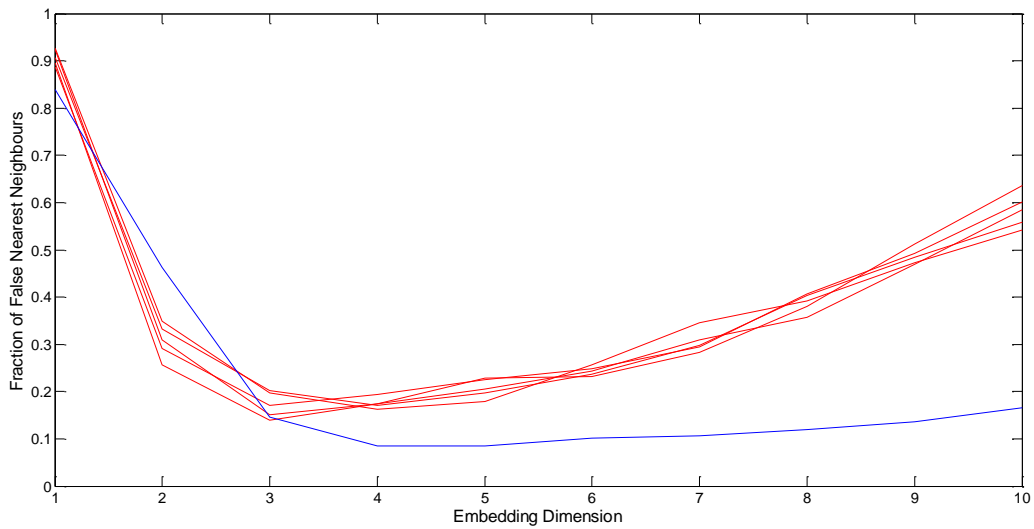
988



989

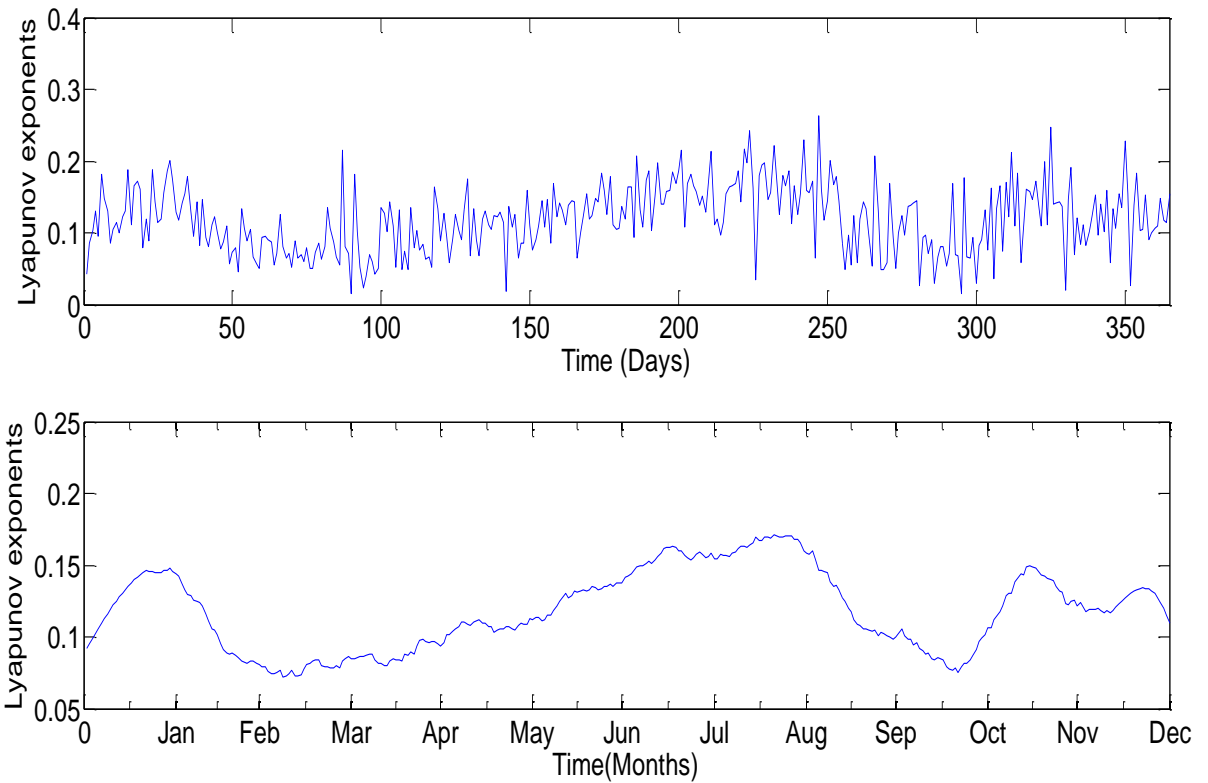
990 Fig 10 Mutual information plotted against time delay for the original detrended data in (blue  
 991 curve) with the mutual information for the surrogate data (red curve) for TEC data measured at  
 992 Lagos for the quietest day of march 2011

993



994

995 Fig 11 Fraction of false nearest neighbours plotted against time embedding dimension for the  
 996 original detrended data in (blue curve) with the mutual information for the surrogate data (red  
 997 curve) for TEC data measured at Lagos for the quietest day of march 20



1000 Fig. 12a Daily variation of Lyapunov exponents for TEC measured at the Enugu station for the  
1001 year 2011 showing the Original data (Upper Panel) and the smoothed Plot of daily variation of  
1002 Lyapunov exponents for TEC measured at the Enugu station for the year 2011 (Lower panel)

1003

1004

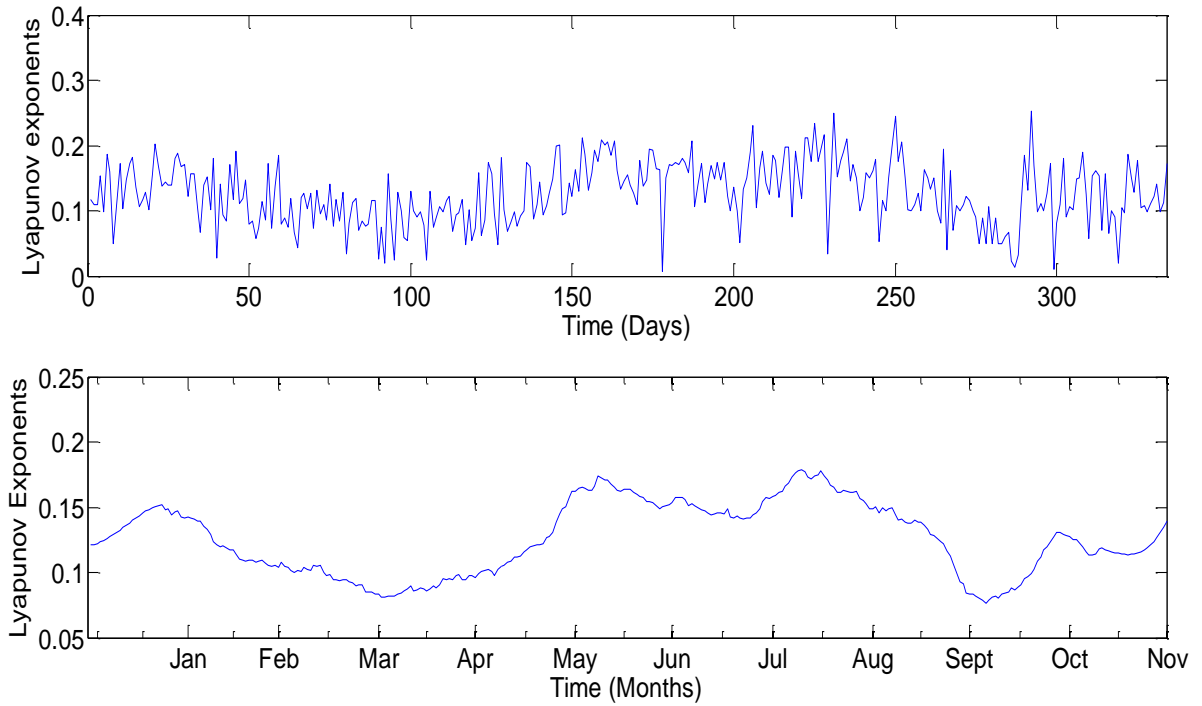
1005

1006

1007

1008

1009



1010

1011

1012 Fig 12b Daily variation of Lyapunov exponents for TEC measured at the Toro station for the  
 1013 year 2011 showing the Original data (Upper Panel) and the smoothed Plot of daily variation of  
 1014 Lyapunov exponents for TEC measured at the Toro station for the year 2011 (Lower panel)

1015

1016

1017

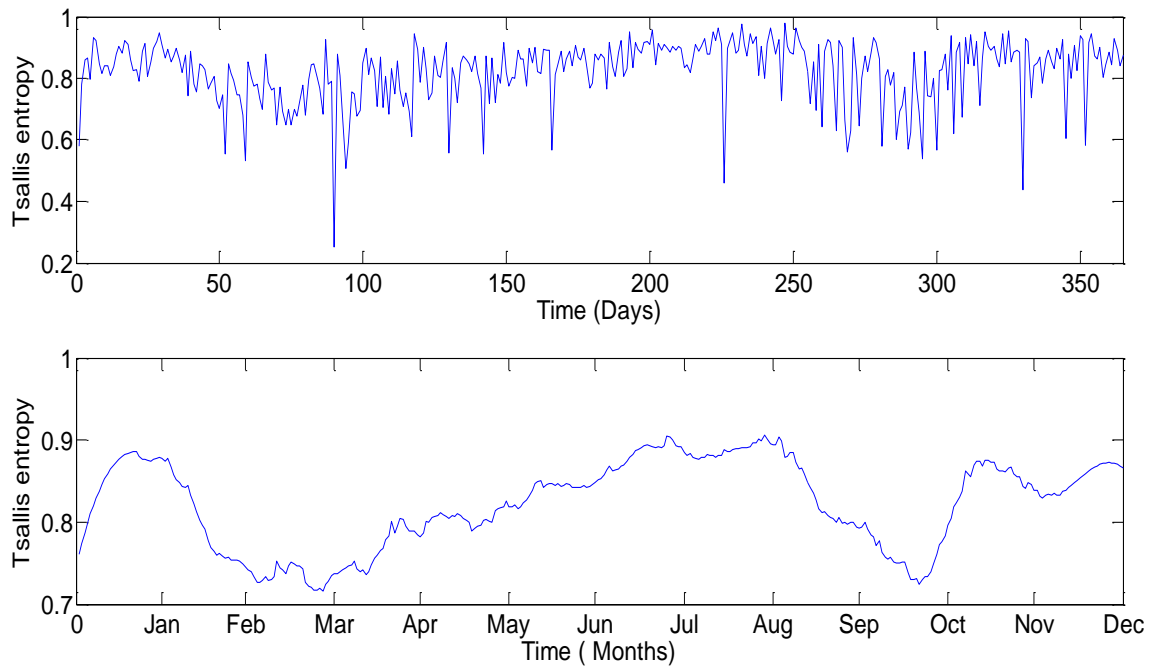
1018

1019

1020

1021

1022



1023

1024 Fig. 13a Daily variation of Tsallis entropy for TEC measured at the Enugu station for the year  
 1025 2011 showing the Original data (Upper Panel) and the smoothed Plot of daily variation of  
 1026 Lyapunov exponents for TEC measured at the Enugu station for the year 2011 (Lower panel)

1027

1028

1029

1030

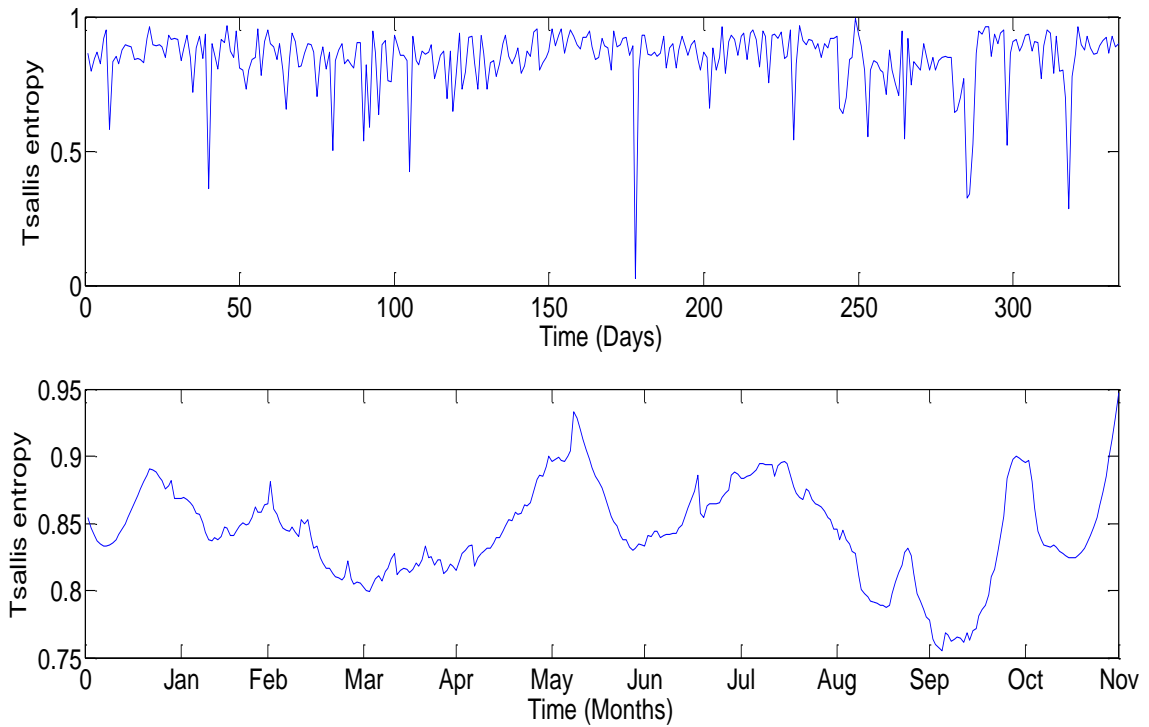
1031

1032

1033

1034

1035



1036

1037

1038 Fig. 13b Daily variation of Tsallis entropy for TEC measured at the Toro station for the year  
 1039 2011 showing the Original data (Upper Panel) and the smoothed Plot of daily variation of  
 1040 Lyapunov exponents for TEC measured at the Enugu station for the year 2011 (Lower panel)

1041

1042

1043

1044

1045

1046

1047